

CZECH TECHNICAL UNIVERSITY IN PRAGUE

FACULTY OF MECHANICAL ENGINEERING

DEPARTMENT OF MECHANICS, BIOMECHANICS AND  
MECHATRONICS

---



MECHANICAL EXCITER FOR EXPERIMENTAL MODAL  
ANALYSES

THESIS

## I. OSOBNÍ A STUDIJNÍ ÚDAJE

Příjmení: **Petrík** Jméno: **Tomáš** Osobní číslo: **409605**  
Fakulta/ústav: **Fakulta strojní**  
Zadávací katedra/ústav: **Ústav mechaniky, biomechaniky a mechatroniky**  
Studijní program: **Strojní inženýrství**  
Studijní obor: **Mechatronika**

## II. ÚDAJE K DIPLOMOVÉ PRÁCI

Název diplomové práce:

**Mechanický budič pro experimentální modální analýzu**

Název diplomové práce anglicky:

**Mechanical excitator for experimental modal analyses**

Pokyny pro vypracování:

1. Seznamte se s metodami experimentální modální analýzy a z toho vyplývajícími požadavky na zdroje budící síly
2. Proveďte rešerši existujících řešení pro modální buzení
3. Navrhněte vlastní konstrukci modálního budiče na mechanickém principu
4. Sestrojte funkční vzorek navrženého budiče a ověřte experimentálně jeho funkčnost
5. Na základě výsledků experimentů proveďte kinematickou a dynamickou optimalizaci konstrukce

Seznam doporučené literatury:

MCCONNELL, Kenneth G. Vibration testing: theory and practice. John Wiley & Sons, 1995.  
BILOŠOVÁ, Alena. Aplikovaný mechanik jako součást týmu konstruktérů a vývojářů: část modální zkoušky. Ostrava: Vysoká škola Báňská ? Technická univerzita Ostrava 2012  
SOBOTKA, Petr. Implementace algoritmů experimentální modální analýzy. Praha: Ústav mechaniky, biomechaniky a mechatroniky, ČVUT v Praze 2012

Jméno a pracoviště vedoucí(ho) diplomové práce:

**Ing. Pavel Steinbauer, Ph.D., odbor mechaniky a mechatroniky FS**

Jméno a pracoviště druhé(ho) vedoucí(ho) nebo konzultanta(ky) diplomové práce:

Datum zadání diplomové práce: **26.04.2018** Termín odevzdání diplomové práce: **17.08.2018**

Platnost zadání diplomové práce: \_\_\_\_\_

Ing. Pavel Steinbauer, Ph.D.  
podpis vedoucí(ho) práce

prof. Ing. Milan Růžička, CSc.  
podpis vedoucí(ho) ústavu/katedry

prof. Ing. Michael Valášek, DrSc.  
podpis děkana(ky)

## III. PŘEVZETÍ ZADÁNÍ

Diplomant bere na vědomí, že je povinen vypracovat diplomovou práci samostatně, bez cizí pomoci, s výjimkou poskytnutých konzultací.  
Seznam použité literatury, jiných pramenů a jmen konzultantů je třeba uvést v diplomové práci.

\_\_\_\_\_  
Datum převzetí zadání

\_\_\_\_\_  
Podpis studenta

# Annotation sheet/Anotační list

Author's name/Jméno autora: Tomáš PETRÍK

Title of thesis/Název DP: Mechanický budič pro experimentální modální analýzu

English title of thesis: Mechanical exciter for experimental modal analyses

Year: 2018

Field of study/Odbor studia: Strojní inženýrství

Department/Ústav: Department of mechanics, biomechanics and mechatronics

Supervisor/Vedoucí: Ing. Pavel Steinbauer, Ph.D.

Consultant/Konzultant:

Bibliographic data/ number of pages/počet stran: 83

Bibliografické údaje: number of figures/počet obrázků: 47

number of tables/počet tabulek: 0

number of attachments/počet příloh: 1

Klíčová slova: mechanický budič, experimentální modální analýza, optimalizace, excentr, buzení

Keywords: mechanical exciter, experimental modal analyses, optimization, eccentric, excitation, shaker

Anotace: Tato práce se zabývá budiči pro modální analýzu a to zejména budičem mechanickým. Je zde navržena konstrukce mechanického budiče a tento budič je následně experimentálně analyzován. Na základě výsledků experimentální analýzy je provedena kinematická a dynamická optimalizace budiče. Finální návrh budiče je proveden tak, že lze nastavovat mechanické parametry budiče pro každou frekvenci.

Abstract:

This diploma is about exciters for modal analysis. Namely about mechanical exciters. There is a proposed design which is then experimentally analyzed. With these results from the experiments is then done kinematic and dynamic optimization of the exciter. The final design is executed in such a way that mechanical parameters can be set for each frequency separately.

## DECLARATION

I declare that I wrote this diploma named

*"Mechanical exciter for experimental modal analysis"*

on my own and all literature and external sources are listed in the list of literature.

In Prague 17. 8. 2018

.....

Tomáš Petřík

## ACKNOWLEDGMENT

I would like to give special thanks to my supervisor Ing. Pavel Steinbauer, Ph.D for his valuable advices, willingness and patience during the whole work. My huge gratitude also goes to my parents and grandparents which supported me during my whole studies.

# Content

Content.....	7
1. Introduction .....	9
Motivation and goal of the thesis .....	10
2. Modal Analysis.....	11
2.1 Basic terms and principles .....	11
2.2 Mathematical description .....	13
2.2.1 Systems with one degree of freedom (SDOF) .....	13
2.2.2 Model with more degrees of freedom (MDOF).....	14
2.3 Experiment – modal test.....	16
3. Exciters .....	18
3.1 Mechanical exciters.....	19
3.1.1 Impact hammer .....	19
3.1.2 Shaker with unbalanced mass .....	20
3.1.3 Direct drive shaker .....	22
3.2 Piezoelectric actuator .....	23
3.3 Electrodynamics shaker .....	24
3.4 Electromagnetic exciter.....	25
3.5 Hydraulic shakers.....	26
3.6 Pneumatic shakers .....	26
3.7 Special excitation .....	27
3.8 Summary .....	27
4. Mechanical shaker design and manufactured.....	28
4.1 3D model.....	28
4.1.1 Functional description.....	29
4.2 Real manufactured model .....	31
4.2.1 Parameters of real device.....	31
4.3 Mathematical and physical model.....	32
4.4 Experiment .....	33
4.4.1 Description of experiment .....	34
4.4.2 Equipment specification .....	35

4.4.3	Data processing.....	36
4.4.4	Measurement and design conclusions.....	40
4.5	Experiment summary .....	41
5.	Optimization .....	42
5.1	Optimization of mechanics .....	42
5.1.1	Model for optimization.....	43
5.1.2	Equilibrium point.....	44
5.1.3	Optimization parameters.....	45
5.1.4	Mathematical optimization .....	47
5.2	Complete model .....	60
5.2.1	Comparison.....	64
6.	Design.....	66
6.1	Eccentric.....	66
6.2	Adjustable parameters .....	69
6.2.1	Adjustable stiffness $k_b$ .....	69
6.2.2	Predeformation $r_0$ .....	70
6.2.3	Eccentricity $e$ .....	71
6.3	Drive.....	74
6.4	Design summary.....	77
7.	Conclusion .....	78
	Reference .....	80
	List of figures.....	82
	Appendix A.....	84



# 1. Introduction

History of construction is long and from beginning we know one sad thing, accidents happened. We cannot absolutely prevent accidents, but we can minimize them. Dimensioning was at first about experiences and estimations only. Later, with advancement of mathematics and all sciences, engineers begun use exact approach with calculations. Statics problems was explored and solved relatively early and satisfactorily. However, dynamics problems were long time on the brink of interest and unexplored.

Dynamics part of testing structure has begun to be researched more or less since half of 19<sup>th</sup> century. Today we are available methods and technologies, which allows solve many problems, problems which was insoluble before. Exploring the dynamics behavior of structures is today developed theoretically and experimentally too. Today it is used almost in all parts of industry under the name vibrations analysis (testing) or (preferred by author) *Modal analysis* (testing).

In theoretical approach we can use FEM methods, calculate mass, stiffness and from that is possible calculate eigenvalues and eigenvectors which are corresponding with natural frequencies and normal mode shapes. In experimental area, modal tests are provided on real part or system. It is for example for measurement of properties or verification of calculated data. System (or component) is excited first and from measured data are determined properties of system (component).

Excitation is typically provided by impulse hammer (smaller and solid components with linear behavior) or by exciter/shaker. Impulse hammer is used for excitation by one hit in wide range input spectrum. Shakers are typically used for nonlinear and very heavy systems. Shakers are based on many principles with many possibilities of using. This thesis is focused mostly on mechanical shakers and optimization of them.

## **Motivation and goal of the thesis**

As it was mentioned earlier nowadays dynamic testing is becoming a common practice. It is used mainly for either testing the properties or output control. That why it is necessary to study it further. One of the key elements in modal testing are exciters. There many kinds of them but all of them have one thing in common – their high price. Given that the need to use EMA is quite frequent it would be good to have some inexpensive exciter with wider range of application. Either for taking measurements in the whole range of the spectrum or just for testing properties on only few frequencies for output control.

The goal of this diploma was to understand modal analysis namely in the area of exciting the object. Furthermore, to gain some idea about exciters and their properties.

Then based on this information, to design and construct a small mechanical exciter and experimentally confirm its properties and operation. It was also important to introduce myself to the process of experimental measurements during my experiments.

After obtaining the information from the measurement the goal was to determine the requirements on changes in the construction.

These requirements should not regard only the construction itself, but the kinematic and dynamic optimization should come from these observations.

Last goal was to propose designs of individual nodes of the mechanical shaker and evaluate their benefits and downsides.

## 2. Modal Analysis

The simplest definition of what modal analysis is can be: “what happens in the system when it is loaded by vibrations”.

But in fact, it is much more complicated and complex problem. There are two approaches to modal analysis. Analysis of virtual model using finite element method or modal testing.

### 2.1 Basic terms and principles

Modal analysis is part of dynamics which deals with description of oscillating behavior and oscillating properties of a system. It is dissecting the behavior into a series of modal contributions. Mathematically speaking – creating a model of a system described by set of differential equations that can be transformed into a system of independently solvable differential equations. In picture 201 you can see this transformation which is then expressed in equation 2.1.

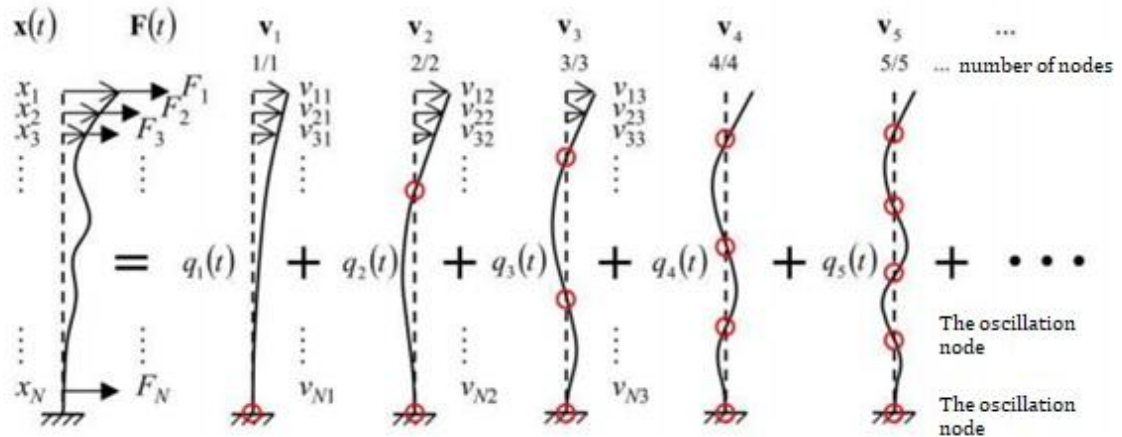


Fig. 201 - Visualisation of modal decomposition[16 pg. 9]

$$x(t) = v_1 q_1(t) + v_2 q_2(t) + v_3 q_3(t) + v_4 q_4(t) + v_5 q_5(t) + \dots \quad (2.1)$$

These differential equations describing the system are characterized by mass matrix, stiffness matrix and damping matrix. After the modal transformation we get

independent differential equations defined by eigenvalues and eigenvectors. The core of modal analysis is finding these eigenvectors – normal modes shape  $v_n$  and eigenvalues  $\lambda_n$ . These numbers and vectors are defined by natural frequencies and dampening.

Knowing these values can solve a lot of technical problems. We can set the system in such a way to resist excitations and therefore not to excessively vibrate. We can also visualize normal modes for given frequencies and from them find sources of unnecessary noise and such.

These values can be obtained using two approaches, theoretical or practical.

The first one is mathematical modeling of systems (simulations). For these one needs to know global matrixes of stiffness (stiffness matrix), mass (mass matrix) and dampening (dampening matrix). Thanks to the advancements in computer science this approach is commonly used nowadays. Problems are usually solved in FEM software like Abaqus or ANSYS.

The second approach is experimental. It combines modal analysis data acquisition with further analysis. In an industrial application, the complete process is often referred to as modal testing and analysis, or experimental modal analysis. By experimental measurements we are measured discrete transfer function. From the discrete transfer function, we determine the parameters of the continuous function  $H(\omega)$ . Transfer function is expressed by equation:

$$H(\omega) = \frac{X(\omega)}{F(\omega)} \quad (2.2)$$

In order to obtain transmission, it is necessary to excite with force source that is capable of operating at wide range, sufficiently strong and capable of keeping the exciting force stable in the whole range.

The advantage of experimental modal analysis is the possibility of testing a system of any complexity, which would be hard, sometimes even impossible to model. Nevertheless, it has its limits. In order to be able to perform modal testing on a system, the system must satisfy the condition of linearity (superposition, homogenous, reciprocal), causality and time invariance.

## 2.2 Mathematical description

The real system (continuum) is replaced by discretized model with finite number of points in which can be focused main properties of the system (mass, stiffness, dampeners). Each of those points can have from 1 to 6 degrees of freedom. Next, we shall assume that each nodal point shall have only 1 degree of freedom and it will be in the direction of the exciting force. First, we will determine the equations for system with 1 degree of freedom (SDOF) which can be applied to only negligible amount of real systems. However, systems with more degrees of freedom (MDOF) and their properties can be then described as a superposition of many SDOF models.

### 2.2.1 Systems with one degree of freedom (SDOF)

Such system can be described as a mass with a spring and a dampener. This dampener can have various characteristic. For the simplicity let's assume a structural damping. This has only a limited usage but for an introductory visualization is satisfactory. More complicated dampening system will be discussed at the MDOF system.

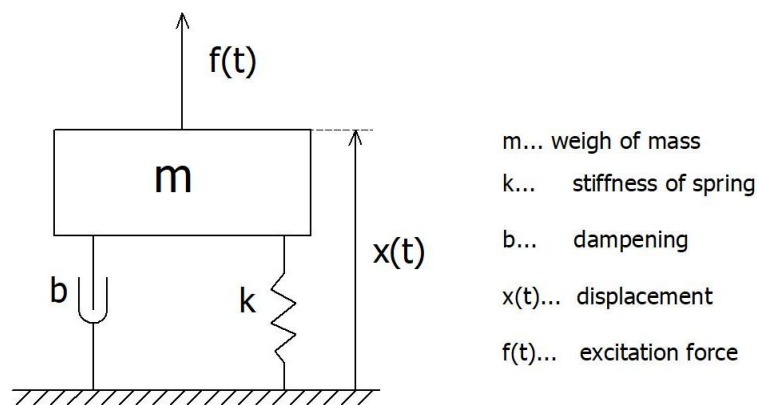


Fig. 202 - SDOF Model

In this model the dampening force is proportional to the velocity of the motion by a constant  $b=[\text{kg/s}]$ . The mathematical model can be then expressed as differential equation of second order:

$$m\ddot{x}(t) + b\dot{x}(t) + kx(t) = f(t) \quad (2.3)$$

More common form of this equation is:

$$\ddot{x}(t) + 2\xi\omega_n\dot{x}(t) + \omega_n^2x(t) = \frac{1}{m}f(t) \quad (2.4)$$

Where  $\omega_n$  is the natural frequency and  $\xi$  is the dampening ratio. After performing the Fourier transformation, we would get a frequency model with only limited usability.

### 2.2.2 Model with more degrees of freedom (MDOF)

System with more degrees of freedom can be graphically interpreted as is show in picture 203. For mathematical description of this system we need a set of interconnected differential equations.

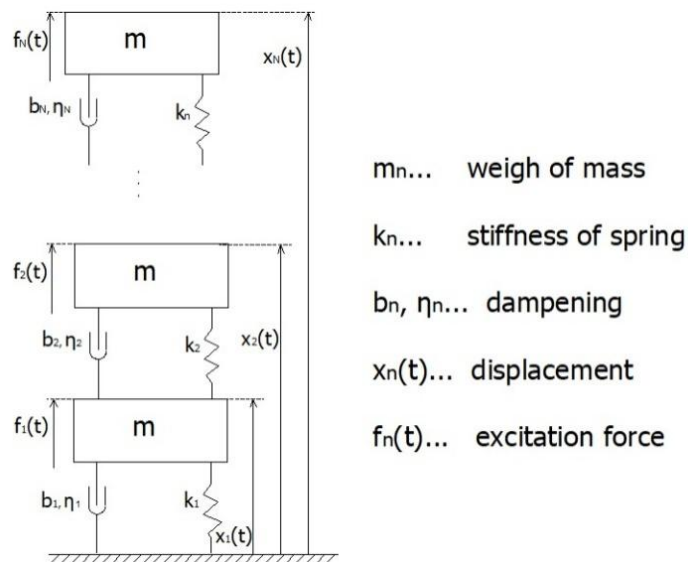


Fig. 203 - MDOF system

As you can see in the picture the MDOF system is just n SDOF systems put together. For describing such system, using matrixes seems as the most reasonable approach. But

in this case, we are going to use although complicated but more usable model with proportional hysteresis dampening, where the dampening has complex character.

$$\underline{M}\ddot{\vec{x}}(t) + [\underline{K} + i\underline{H}]\dot{\vec{x}}(t) = \vec{f}(t) \quad (2.5)$$

The model is described by the equation (2.5) where these terms are present:

- M ... mass matrix
- K ... stiffness matrix
- H ... (complex) dampening matrix

In order to obtain the final equations, we need to do a modal transformation any many other modifications. But this essay is not about the theoretical part of EMA and so I will put here just the finished transfer function. This function can be written as [11pg. 79]:

$$H(\omega)_{rs} = \sum_{n=1}^N \frac{\Phi_{n_s}^* \Phi_{n_r}}{\omega_n^2 (1+i\eta_n) - \omega^2} = \sum_{n=1}^N \frac{A_{n_{rs}}}{\omega_n^2 (1+i\eta_n) - \omega^2} \quad (2.6)$$

- r ...index of the excited point
- s ...index of the geometry point which satisfy the transfer function
- n ...index of mode (n<sup>th</sup> degree of freedom)
- $\Phi_{n_{s,r}}$  ... normalized normal mode shape
- $\omega_n$  ... natural frequency
- $A_{n_{rs}}$  ... modal constant
- $\eta_n$  ... dampening constant

At first glance it is obvious that the transfer function of the whole model is basically sum of individual points. In the equations there are the sought terms which of course are dependent on each other. If the system is excited on its natural frequency  $\omega_n$

the dominant shape of the vibration is the one given by the normal mode  $\Phi_{n,s,r}$ . For determining these parameters, we should theoretically determine frequency transfers over the interval  $(0,\infty)$ . But that is not feasible, and we are limiting the interval to some finite value. The interval is usually decided by operation of the system. With these limitations we need to be careful about “boundary conditions” and expand the transfer function with additional terms. For more information about the theory behind it look at [12 pg.95].

## 2.3 Experiment – modal test

In modal testing are used so called shakers. Shaker is an equipment which is used for excitation of the system. System (machine, frame, etc....) is excited with specific frequency (frequencies) and the signal is then analyzed.

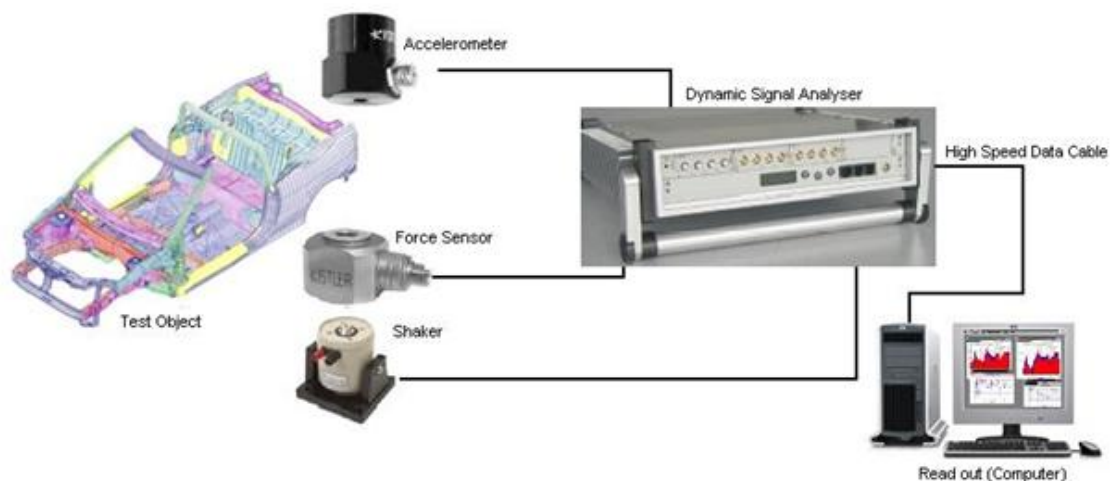


Fig. 204 –Simple exhibition of structure of experimental set up for EMA [2]

In picture 204 is a showcase of elements used for EMA. Now we shall go through important aspects of the experiment:

- **Determining the point net** – these are the points that discretizes the continuum. Exactly in these points is the system excited and the response measured.
- **Mounting of the object** – the object needs to be mounted only lightly - e.g. Suspended only on very soft springs - so the properties of the system are affected to a minimum.



- **Mean of excitation** – Appropriate frequency band is usually given by the type and operation of the system. So is the type of the signal. According to the maximum parameters it is important to correctly choose the type of exciter.
- **Sensors** – the sensor must be chosen with respect to range (of forces, frequencies, tensions...) and with respect to the system itself. Just like choosing the right exciter and mounting of the system it is important for the detectors as well to affect the system as little as possible. Mainly in terms of added mass (e.g. for small systems it is better to use vibrometers than piezo accelerometer). The most common error is using a sensor with too narrow range. That will cut the signal which will bring a lot of nonsensical frequencies into the measurements. Of course, there are more possible errors.

Two means of measurement are used:

**Rowing response** – In this case the system is excited only in one (or few) point/s and in the remaining points the response is measured. Exactly for this type of measurement are used shakers and for the measurement it is important to avoid nodal points.

**Rowing excitation** – For this kind of measurement is usually used an impulse hammer. The excitation is done in many points and the response is measured in one (or few) point/s.

Using these methods allows for linear property known as reciprocity.

### 3. Exciters

Exciter is the basic element for modal analysis. It is the source of exciting force for every modal test. There are many types of tools and devices to excite a system for modal analysis. Typically, they can be sorted by operational principles like for example:

- Mechanical exciter
  - Impact hammer
  - Direct drive shaker
  - Shaker with unbalanced mass
- Piezoelectric actuator
- Electrodynamics shaker
- Electromagnetic exciter
- Hydraulic shakers
- Pneumatic shakers
- Special excitation

For exciting a system for modal analysis, it is important to keep in mind:

- Correct points of excitations
- Adequate excitation
- Frequency range of excitation
- Equivalent magnitude of force for each frequency.

The properties of the exciter must come from the requirements mentioned above.

## 3.1 Mechanical exciters

As a mechanical exciter can be called many things so I will list just few basic ones.

### 3.1.1 Impact hammer

Also called impulse hammer. It is probably the most common type of exciting device. It is very good for impact excitations, a technique that was developed in 1970s (Halvorsen and Braun (1997[3])).

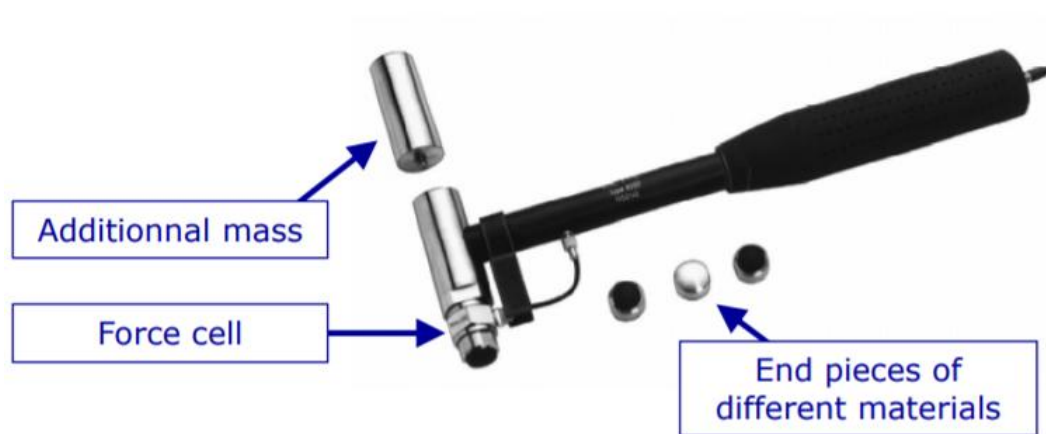


Fig 301 - Impact hammer [8]

The hammer is shown in picture 301. It consists of the body of the hammer, an additional mass, a force cell and a rounded end which can be made out of different materials (in order to not to damage the system). Its size can range from grams up to 10 kg with long handle.

The mass of the hammer must be proportionate to the system (approx.  $m_{\text{system}}=25*m_{\text{hammer}}$ [10]) otherwise the system will not be excited enough in terms of force and frequency. In another word the maximum derived frequency is lower and so the maximum excited frequency is also lower.

The radius of the hammer's end quite significantly affects the excited frequency band in an indirect proportion. The radius of the end is usually not less than 10 mm.

Parameters[10]:

- Mass: up to 1000 kg
- Frequency: to 5 kHz
- Force: perpendicular
- Pulse signal

Pros:

- Low cost
- Variability (easy to excite multiple spots and easy to change the excited spot)
- Easy access to a large number of excitation points
- No mass is added to the system
- Reliability
- Speed and complexity of evaluation of measured data
- Open for improvisations

Cons:

- Limited system mass
- Possibility of excitation to the non-linear region (ratio between peak and effective value of a signal)
- Uncertainty in the repeatability
- Uncertainties about the location of the application point, the direction and the amplitude of the force

### 3.1.2 Shaker with unbalanced mass

It's a reaction type where two unbalanced masses rotate in opposite directions in order to generate a dynamic reaction force that acts only in one direction.[3]

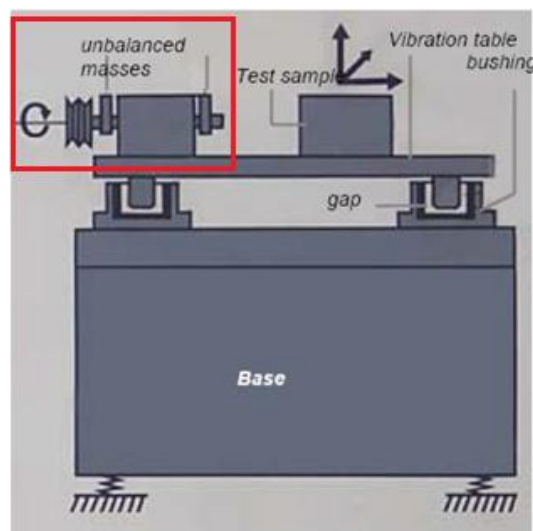


Fig. 302 -Experimental equipment of company Robert Bosch GmbH [4]

In picture 302 is shown configuration where the exciter (in red box) is assembled on table which can move in one direction. This is just one of many possible configurations. The exciter can be for example mounted onto the studied system.

Advantage of this type of mechanical shaker is the possibility to set the force for every frequency by setting position of the unbalanced mass. However, this is not possible during operation but only in standstill machine. Also, the amplitude can't be exactly set.



**Fig. 303 -Vibration motor with open chamber for unbalance mass [5]**

In picture 303 is exciter with unbalanced mass on only one shaft. In this execution the force effect is on the rotation vector creating quite complicated motion which can be used only for determining the natural frequencies. That is why the previous alternative with directed force effect is more common.

Parameters[10]:

- Mass: up to  $10^7$  kg
- Frequency: up to 100 Hz
- Force can act in any direction
- Sinusoid signal

Pros:

- Large force effect
- Force effect can be calculated – doesn't have to be measured
- Force effect can be set for any frequency

Cons:

- Large dimensions
- Difficult implementation
- Amplitude increases with rotations
- Only harmonic forces

### 3.1.3 Direct drive shaker

This type works on similar principle like a crank shaft. But the crank is usually replaced by eccentric. Typically, these are executed as vibrating tables. The excitation force is created as an inertial force on the mass of the table and mass of the system.

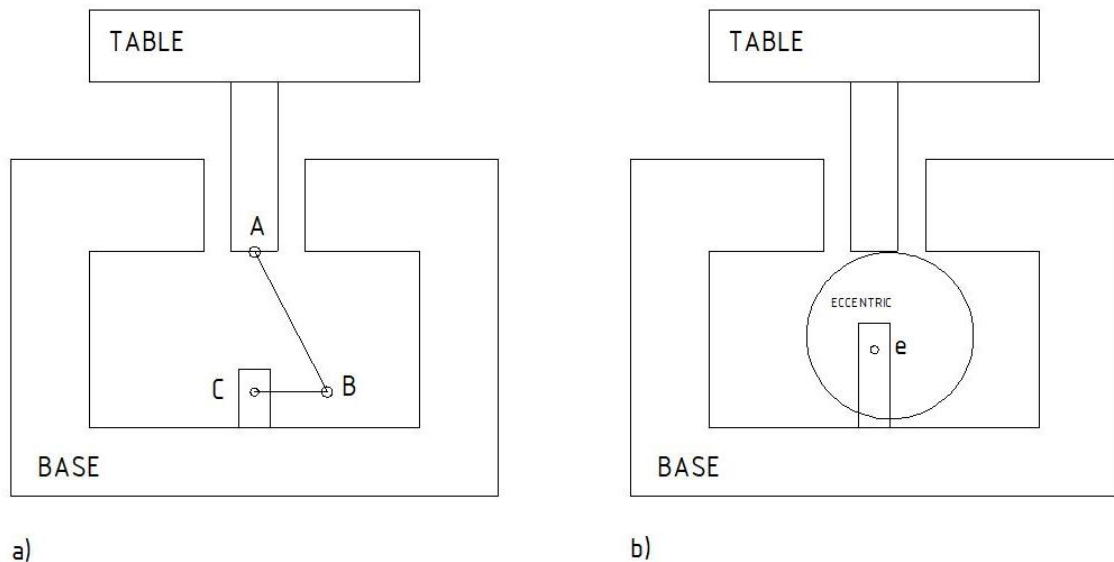


Fig. 304 - Direct-drive shaker a) crank b) eccentric

In picture 304 are diagrams of possible execution of direct drive shakers. In picture 304a you can see the crank shaft execution and in picture 304b is the eccentric execution. The real device then can look like a combination of those two.

Parameters[10]:

- Mass: up to 100 kg
- Frequency: up to 1 kHz
- Force can act in any direction
- Sinusoid signal

Pros:

- Amplitude can be set by the eccentricity
- Relatively large force effect
- Force effect can be set for any frequency
- Force effect can be calculated

Cons:

- Amplitude increases with rotations
- Larger dimensions
- Only harmonic forces

### 3.2 Piezoelectric actuator

A typical piezo-actuator is usually used, which works on the piezo electric principle (simply put – a table of nanocrystal silicon changes shape according to applied voltage.). Piezoelectric shares are typically used where you need high frequency but for the cost of smaller amplitudes.

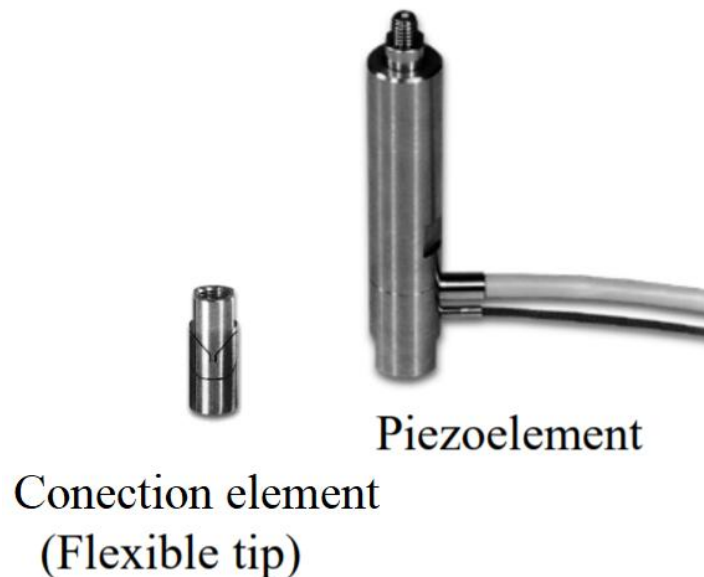


Fig. 305 - Piezo actuator for modal excitation with connection element [10]

In picture 305 you can see one possible realization of piezo-element used for modal analysis.

Parameters[10]:

- Mass: up to 100 kg
- Frequency: up to 50 kHz
- Force can act in any direction – in the axis of the crystal
- Signal can be set with a program

Pros:

- Large dynamics
- Control over the location of the application point and the direction of the force

Cons:

- Only pressure stress in the axis
- Large hysteresis
- Large length drift
- Frequency band is limited by the amplifier

### 3.3 Electrodynamic shaker

It is probably the most common type of exciters. A coil is moving in a magnetic field created by a permanent magnet or DC electromagnet (larger shakers), creating an oscillating force.

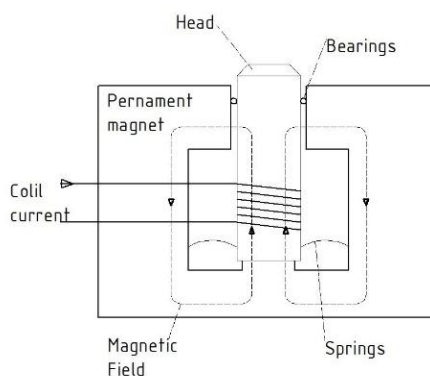


Fig. 306 - Principle diagram of electrodynamic exciter



Fig. 307 – Showcase of electrodynamic exciters [14]

Parameters[10]:

- Mass: up to  $10^4$  kg
- Frequency: up to 10 kHz
- Force can act in any direction – in the axis of the coil
- Signal can be set with a program



Pros:

- Possibility of simultaneous multi-excitation
- Control over the location of the application point and the direction of the force
- Large number of averages = noise reduction

Cons:

- Expensive
- Resonances of the stinger
- Added mass to the structure
- More difficult implementation
- Pliability of the core attachment may have an effect on the measurements.

### **3.4 Electromagnetic exciter**

Magnetic circuit is closing over the measured system. That implies large nonlinearity which leaves the possibility for only small range of oscillations. For its nonlinear behavior is this exciter scarcely used (almost not at all).

Parameters[10]:

- Mass: up to 100 kg
- Frequency: up to 1 kHz
- Force can act in any direction – in the axis of the coil
- Signal can be set with a program

Pros:

- Noncontact connection
- No added mass

Cons:

- Nonlinearity
- Small forces
- Only magnetic materials

## 3.5 Hydraulic shakers

Or more precisely electrohydraulic exciters have their parameters determined by the flow rate and pressure of the hydrogenator and the area of the piston. They allow for simultaneous execution of static (prestress) and dynamic load. That is beneficial where the prestress can affect dynamic properties or geometry.

They also allow for long pulse for creating excitation on large amplitudes. This option is not present at the other exciters with similar dimensions.

They are more commonly used in construction for exciting buildings, bridges, etc.

Parameters[10]:

- Mass: tens of tons
- Frequency: up to 50 Hz, specialized ones can go up to 1 kHz
- Force can act in any direction
- Signal can be set with a program

Pros:

- Large forces and amplitudes
- Possibility for static prestress
- In comparison with electrodynamics they are lighter and more compact

Cons:

- Complicated
- More expensive

## 3.6 Pneumatic shakers

This type of exciters is used only a little when testing mechanical systems. They have their advantages as well as downsides that arise from the technology as it is.

Pros:

- They are “clean”
- Quiet
- Long lifetime

Cons:

- “Soft” (small forces)
- Nonlinear

### **3.7 Special excitation**

Very extreme cases like detonating an explosive or rocket or cutting a support rope and things like that. Usually these are one-time only tests with impulse characteristics of a signal, lower width of excited frequencies and are for exciting systems with large mass.

### **3.8 Summary**

On the market we can find a lot of different types of mechanical exciters. Many of which has been listed in the previous chapter. Currently the most common types of exciters used for modal analysis are electromechanical shakers which have many advantages. Their downside is their high cost.

I was personally more interested in mechanical exciters. They are usually manufactured as tables. Their price doesn't have to be necessarily high although they have one great downside. The excitation force increases as the frequency increases and that is unrequired when doing EMA.

Currently, when EMA is used very often and in many fields from automobile industry to sport equipment testing for output control and so there is this possibility for designing some inexpensive universal exciter. This is a perfect option for mechanical exciters fitted with modern elements like air spring, controlled dampeners, different kinds of actuators, controlled sensors and even some simple AI. Such shaker can be used either for examining properties on a larger frequency scale of a part or only on one or two frequencies which are important for the given part in output control.

The goal of this thesis is to learn in depth about other properties of simple real mechanical exciter, primarily during its construction find out its other problems and limitations and then come up with solutions, which would minimize these problems or possibly eradicate the biggest problem of all: Increase of excitation force with the square of angular velocity.

## 4. Mechanical shaker design and manufactured

Basic idea this part is describe small model of direct drive shaker with eccentric, which was first designed in 3D cad system and then manufactured. This model will be used for trying some measurement practice and for assessment of usability of this simple system and model.

Parameters of shaker:

- Frequency  $0 \div 50$  Hz
- RPM (corresponds to the frequency)  $0 \div 3000$
- Added mass (weight of analyzed system) approx.  $0 \div 5$  kg

### 4.1 3D model

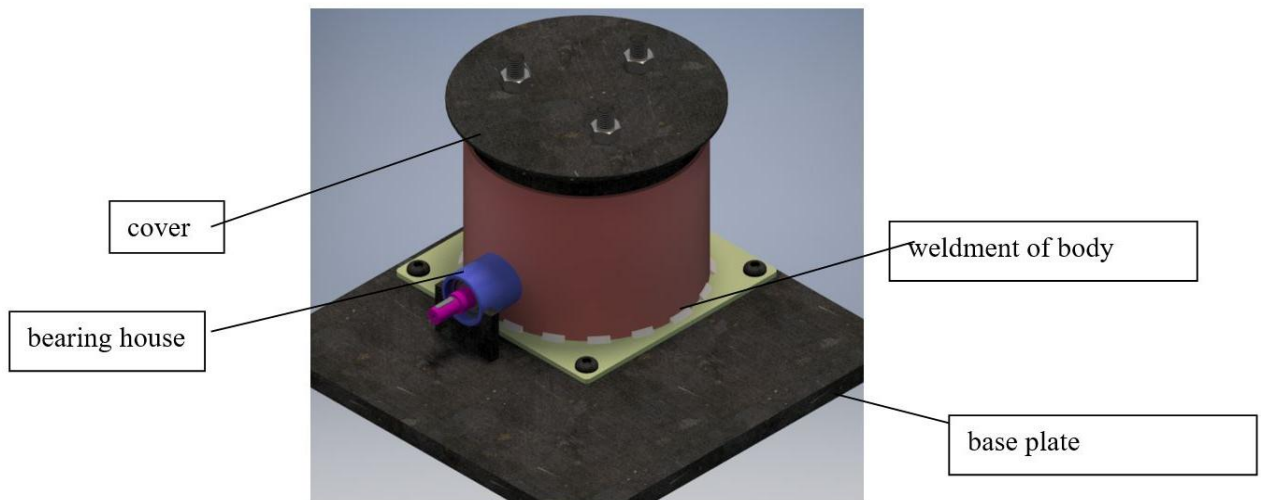


Fig. 401- Global view on 3D model of shaker

In picture 401 is global view on 3D model of shaker. It consists of few basic parts:

- **Base plate** on which is connected everything else.
- **Weldment of "body"** which support bearing house, protect environs in case of accident and support cover in case of non-vertical moving
- **Bearing house** - support shaft which is moving inside the shaker.
- **Cover** is part which „connects excitation" and basic springs. On the cover is also attached analyzed system (in our case only a weight).

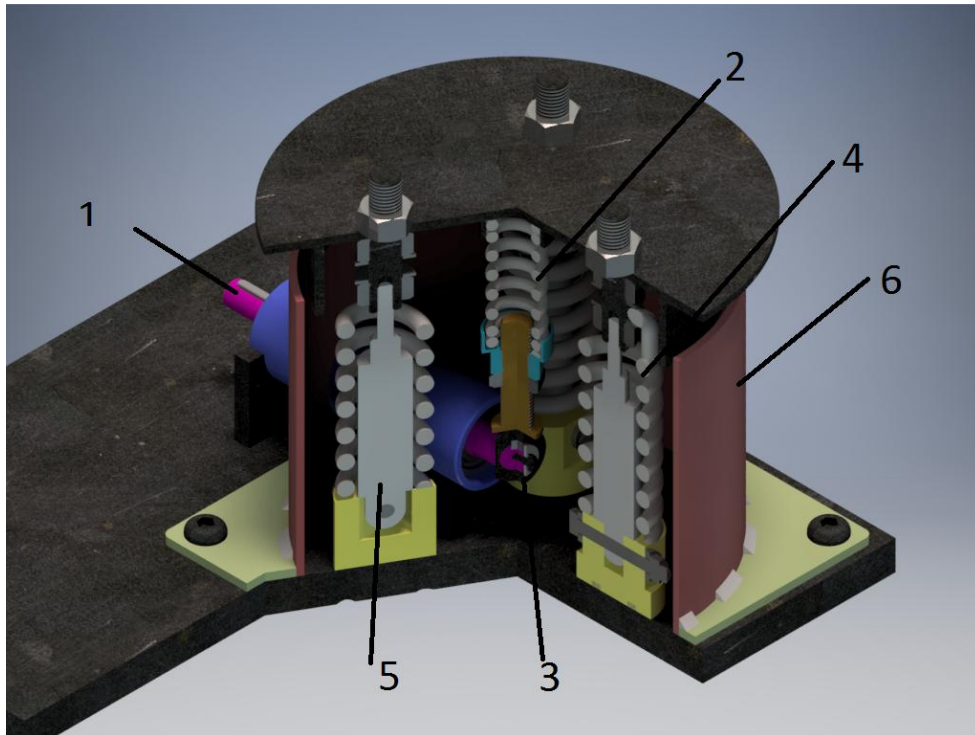


Fig. 402 - Inside view of 3D model with description point

In picture 402 is inside view where is possible see details of construction of shaker. Only damper is not modeled with details because it's bought part. (Pic. 6 is available in appendix in bigger size).

- 1) In coming side of shaft. Here is connected motor by clutch (our case), gear, pulley, ...
- 2) "Excitation spring" - by this spring is supplied energy from eccentric (3) on cover
- 3) eccentric
- 4) Main spring
- 5) Damper
- 6) Weldment of body

#### 4.1.1 Functional description

Shaft is powered by motor and revolves eccentric. Excitation spring is excited by eccentric and is pushing cover which is "kept in place" by main springs and dampers. In words of mechanics is possible describe this system by sketch in picture 403.

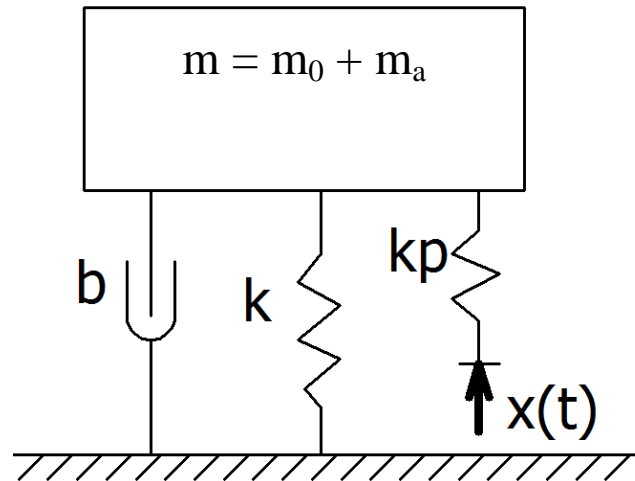


Fig. 403 - Sketch of physical model of shaker

Where:

- $m$  - weight of mass which is accelerated. This consists of weight of parts of the shaker  $m_0$  and weight of added mass  $m_a$ .
- $k$  is 3x spring constant of main spring (number 4 in Fig. 402)
- $kp$  is spring constant of excitation spring (number 2 in Fig. 402)
- $b$  is constant of damping
- $x(t)$  is position of down part of excitation spring like function of time

Naturally  $x(t)$  must satisfy the movement of the eccentric - kinematic excitation is expected. If we will assume 0 position in center of rotation, will be this satisfy this equation:

$$x(t) = e * \sin(\omega * t) + r \quad (4.1)$$

Where:

- $e$  is eccentricity of an eccentric
- $r$  is radius of eccentric

The problem is that would mean that the excitation spring must have free length when the lowest point of the spring support is on the axis of the shaft. That is not the case. It turns out that preload have no influence for dynamic behavior, only for equilibrium position. And therefore, the excitation will be described as:

$$x(t) = e * \sin(\omega * t) \quad (4.2)$$

## 4.2 Real manufactured model

At first glance on picture 404, you can see few changes. Outside support of bearing house is inside because diameter of weldment of body is bigger. Besides in the connection of main springs is sort of changed. The backplates are replaced by big triangular plates which keep all sets springs and dampers together much better. This is impossible to see from picture 404.

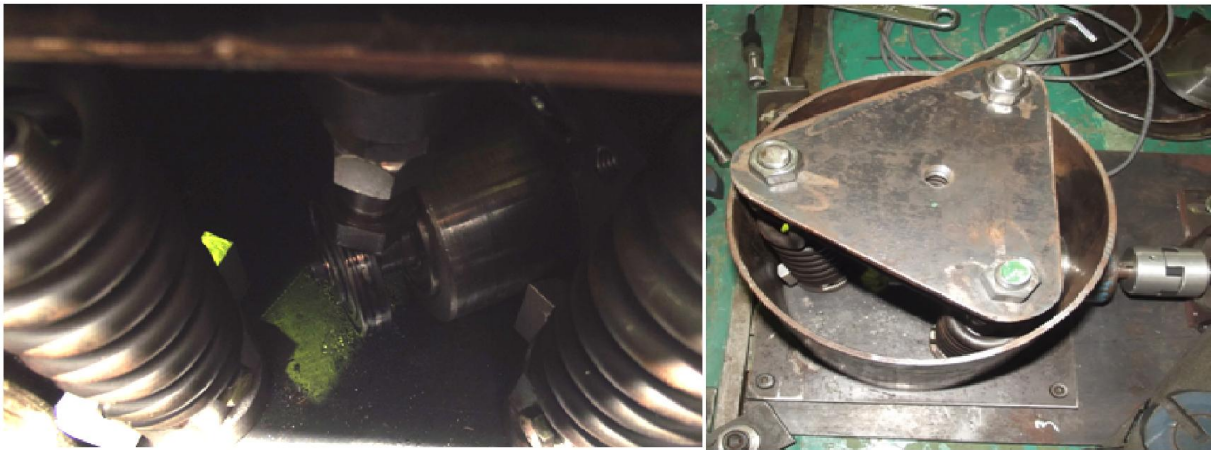


Fig. 404 - Photos of the real model

Also, the cover underwent some changes. Nice annular "piston" was replaced by simple triangular plate.

Furthermore, the simple eccentric was replaced by eccentric from bearing from reduction of friction.

For the connection of the motor and the shaker was used flexible coupling without another transmission.

The changes were caused by using parts that were available.

### 4.2.1 Parameters of real device

When looking at the picture 403, and the equation 4.1, it is obvious that these parameters are essential:

- $m_0 = 3 \text{ kg}$
- $k_p = 140\,000 \text{ N/m}$
- $k = 3 \times 235\,000 = 705\,000 \text{ N/m}$

- $e = 0.00415 \text{ m}$
- $b = 1 \text{ Ns/m}$

### 4.3 Mathematical and physical model

The basic physical model is shown in picture403. Let's follow this model to free-body diagram in picture 405.

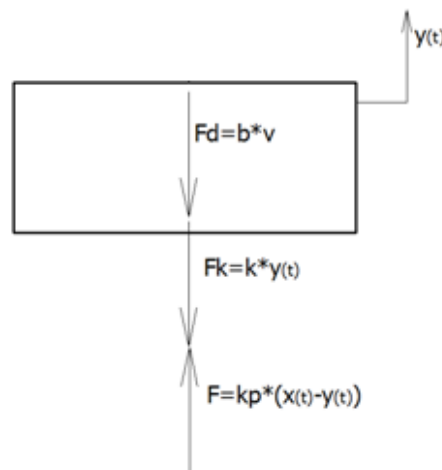


Fig. 405 - Free-body diagram

This free body diagram satisfies this dynamic equation:

$$m\ddot{y} = F - Fd - Fk \quad (4.3)$$

Substitution forces by constants and derivation of  $y$  and mathematical treatment:

$$m\ddot{y} + b\dot{y} + (k + k_p)y = k_p x - mg \quad (4.4)$$

Because measurement of  $y$  is from equilibrium position  $x$  can be replaced from equation 4.2(without  $r$ ) and the result is general mathematical model of shaker, which is represented by differential equation:

$$m\ddot{y} + b\dot{y} + (k + k_p)y = k_p \cos(\omega t) \quad (4.5)$$

Now is possible replaced universal constants by values:

$$m\ddot{y} + 1\dot{y} + (705000 + 140000)y = 140000 * 0.00415 \cos(2\pi f t) \quad (4.6)$$

where  $f$  is frequency of input which will be depend on experiment as well as  $m$ .



Final form of differential equation:

$$m\ddot{y} + 1\dot{y} + 845000y = 581\cos(2\pi ft) \quad (4.7)$$

Now it's necessary evaluate natural frequencies. Theoretical parameters were designed with regard to the difference between operational band and band of natural frequencies.

$$\omega_n = \sqrt{\frac{k}{m}} \quad (4.8)$$

That we can evaluate from equation 4.8. Where  $\omega_n$  is natural frequency of undamped system, k is stiffness of three springs and m is  $m_0$  plus added mass  $\Rightarrow$  m belongs to interval  $\langle 3;8 \rangle$  kg.

After the calculation  $\omega_0$  belongs to interval  $\langle 52;85 \rangle$  Hz. This is a boundary value as the maximal added mass was somewhat different than expected and also the parameters of the real manufactured parts were different. Nevertheless, the experiment was satisfactory.

## 4.4 Experiment

Basic idea why experiment is done is introduce author of the measurement of the dynamic system, processing of measured data and of course check behavior of real system.

In this experiment is measured acceleration and current incoming to **system**, not only to the motor. Next sound is recorded for possibility collation frequency.

The purpose of the current measurement is to determine how rapidly increasing energy consumption depending on the frequency and the added mass.

The purpose of the current measurement is to determine frequency behavior of shaker.

### 4.4.1 Description of experiment

In experiment were set two parameters, input frequency (rotational speed) and mass on shaker.

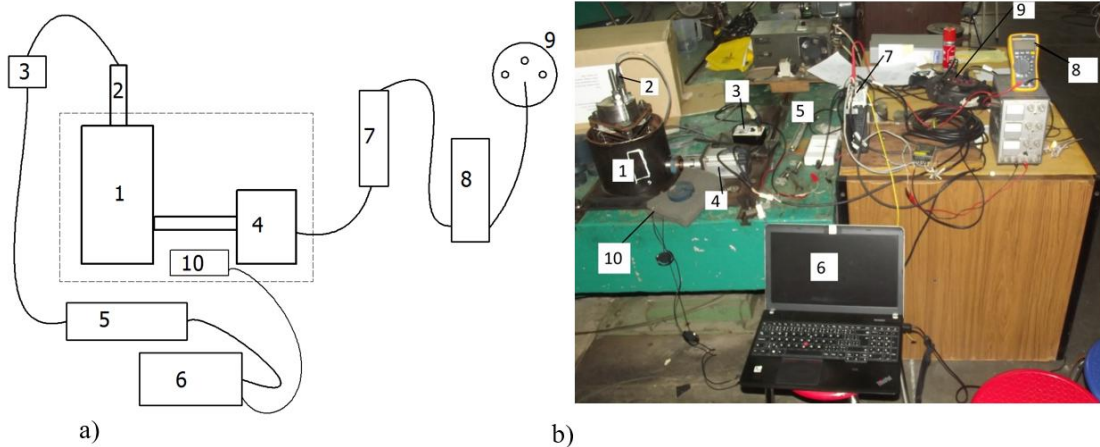


Fig. 406 - Measurement arrangement - a) block schema b) real situation

Frequency was set from 0 to 45Hz (0 - 2700 rpm) with increment approximately 4,167 Hz (250 rpm) and it is done for every added mass from 0 to 5,346 kg (absolute mass from 3 to 8,346 kg) with increment 0,594 kg. Sound was recorded for every measuring.

In picture 406 is show measurement arrangement on this experiment, where:

- 1) Shaker
- 2) Accelerometer
- 3) Amplifier
- 4) Servo motor
- 5) Data acquisition (DAQ) module
- 6) Computer
- 7) Servo driver
- 8) Amperemeter/Multimeter
- 9) Outlet
- 10) Microphone

## 4.4.2 Equipment specification

Accelerometer:

- Sales Technology Inc.
- Type: CMCP 1 200
- Sensitivity: 100 mV/g
- Range: 0,32 - 10k Hz
- S/N 0908042

Amplifier:

- OMEGA Engineering Inc.
- Type: ACC-PS1
- S/N 3043

AC Servo motor:

- Panasonic
- Type: MHMD082G1U
- Output: 750W and 2,4 Nm

DAQ module:

- NATIONAL INSTRUMENTS
- Type: NI USB-6216
- 16 - bit  
16 inputs
- S/N 1603076

Servo driver:

- Panasonic
- Type: MCDHT3520
- S/N P 13080523N

### 4.4.3 Data processing

Theoretical basis for data processing is well known. Nonetheless they are listed in appendix A.

#### *Step one*

In the first step the signals and audio were analyzed by DFT for obtaining information about exactly values of frequency, because on a servo driver it was impossible to exactly set/read a frequency of an input. Imperfections of oscillations were in terms of tens of rpm. That was probably caused by improper mean of control, dimensions and setting of the drive.

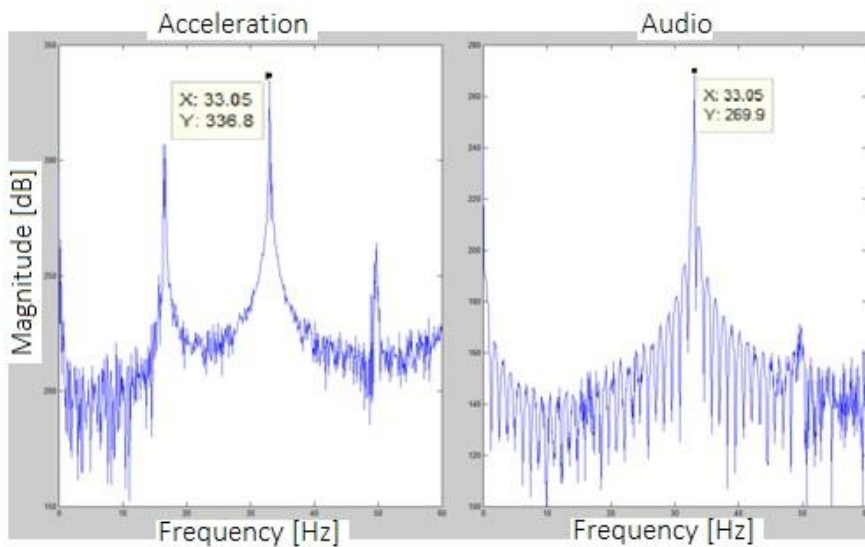


**Fig. 407 - DFT of acceleration (left) and audio (right)**

Example of this analysis is in picture 407. Also, the magnitude was recorded in dB to confirm the measured position of a frequency peak for further analysis and post analysis check.

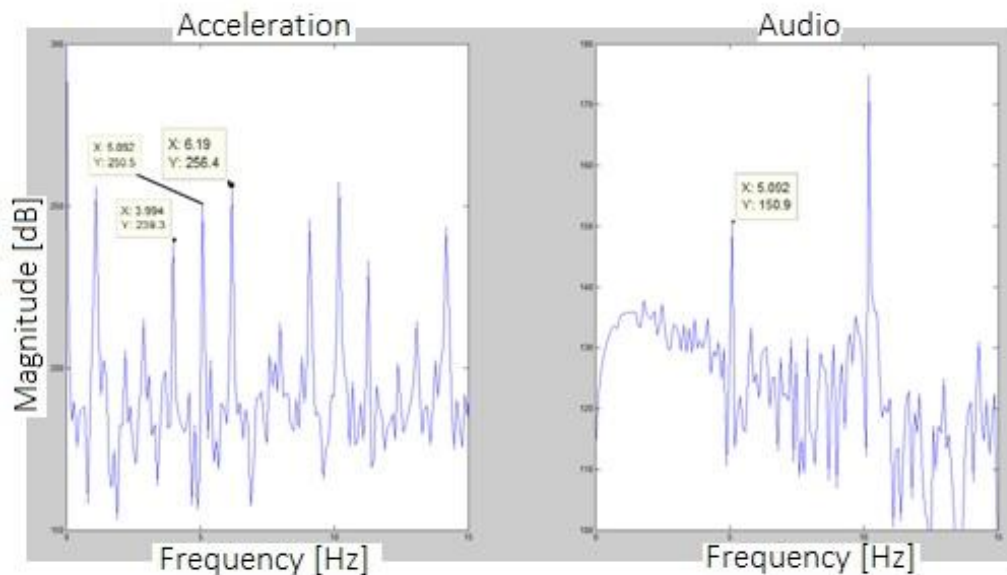


Fig. 408 - DFT of not absolutely clear signal

At first look it may seem unnecessary to perform audio analysis and (if we neglect another information which is possible to get from this analysis) for the clear spectrum like in picture 407, it is true.

But typically, we get signal like in picture 408 where we cannot be sure which frequency is really significant and what is only noise or something unimportant. In such case the audio data are very helpful. The point where two peaks of acceleration and audio overlap is our desired input frequency.

It's worth mentioning that from sound of a mechanism it is possible to get more information than just main operation frequency (or frequencies in a mechanism with transmission) but with this analysis we can get information about defects or some natural frequencies of subsystems.

But for this analysis it is typically necessary to filtered out known frequencies of transmission and apply window functions.

**Step two**

In the second step was analyzed power incoming into the system in relation to the mass and frequency to get an idea of how fast energy demand is growing. First was analyzed situation where frequency was increased with constant mass.

Slope of increasing power from every frequency and single mass											mean	median
slope [-]	5,653	6,219	7,574	7,468	6,771	5,913	5,963	5,815	5,532	6,651	6,3559	6,091
mass [g]	3000	3594	4188	4782	5376	5970	6564	7158	7752	8346		

Fig. 409 Table of slope of increasing power from every frequency and single mass

The results of this analysis are in table in picture 409. Mean slope of power increase is 6,36 but it is not possible to see any relation between slope and mass (the slope doesn't seem to be increasing with increasing mass which might be expected).

Also, increase in power was analyzed for situation where frequency was stable, and mass was increasing. The measurement was not performed. The data were taken from previous measurement. But in this case the data provided no applicable information. Probably because measurement was not performed in one sequence.

### ***Step three***

In the third step was differential equation 4.7 numerically solved for given mass and frequency in order to compare data from model (the equation) and data from accelerometer.

Also, data from accelerometer were processed. That was quite challenging because the sampling frequency for recording was chosen too big (oversampled) and signal contained a lot of noise.

The noised signal was first filtered using two filters, highpass and lowpass filter and then resampled. (Band pass filter did not work well.) In picture 410 is shown one example of signal filtering. The red curve is lowpass filter; the purple curve is highpass filter. Blue peaks are spectrum of not filtered signal and black "+" is the spectrum of the filtered signal.

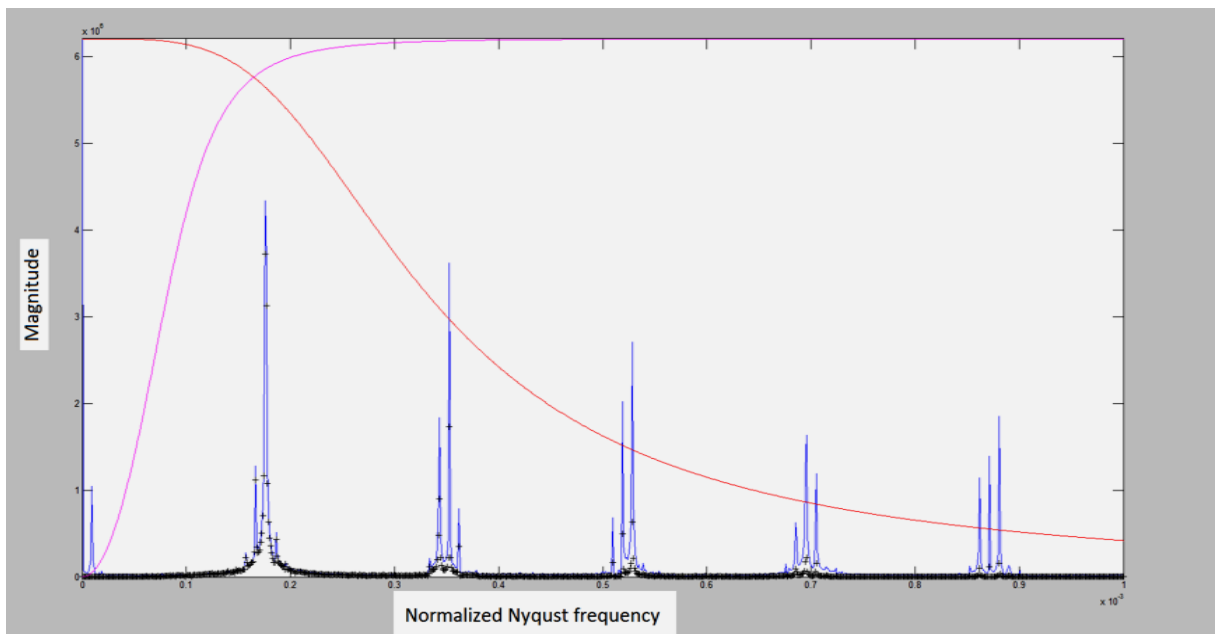


**Fig. 410 - Spectrum with filters**

Filtered signal was fed in to the "cftool" (Curve fitting tool) in MATLAB and interspaced by curve defined as linear combination of sine and cosine wave. This is shown in picture 411 and data under the graph correspond to the properties of the signal from accelerometer.

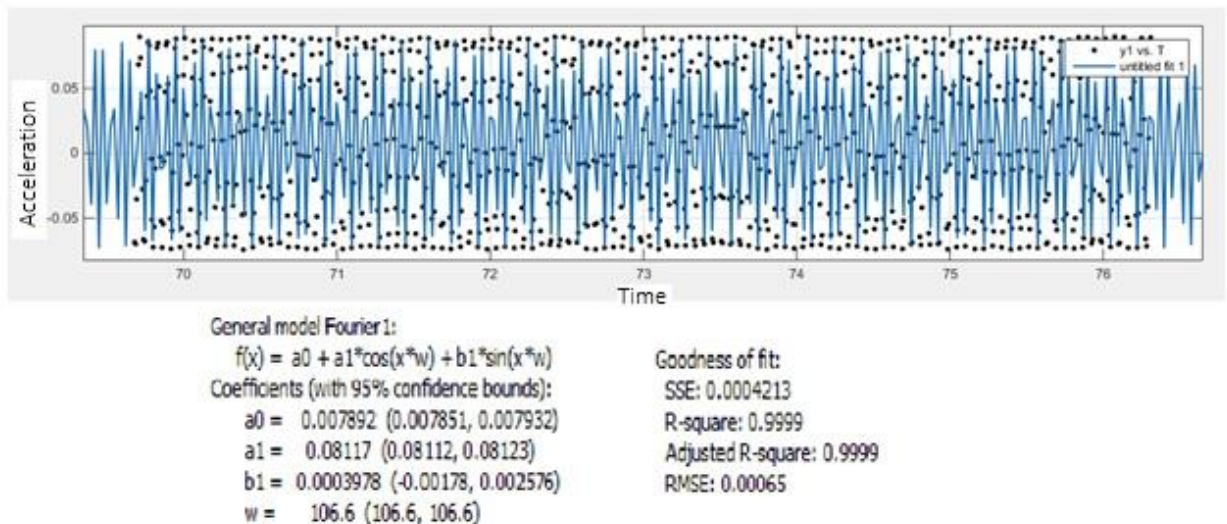


Fig. 411- Approximation of data from accelerometer in CF tool

In picture 412 is in "cftool" shown signal from accelerometer (black) and modeled acceleration (blue). Data under the picture correspond to the modeled acceleration.

Model was created for angular frequency 106,6 rad/sec from DFT and from the signal we are getting 105,6 rad/sec. That means frequency difference of 0,16 Hz. That can be considered quite satisfactory.

Regarding the amplitude signal, which we are also trying to compare, the situation is somewhat more complicated. The percentage difference on the approximation is about 20%. Looking at the peaks it's even more. This difference could be compensated for with the parameter of model dampening. Furthermore, it is obviously given, judging by the shape of the signal from accelerometer, by the character signal being heavily different.

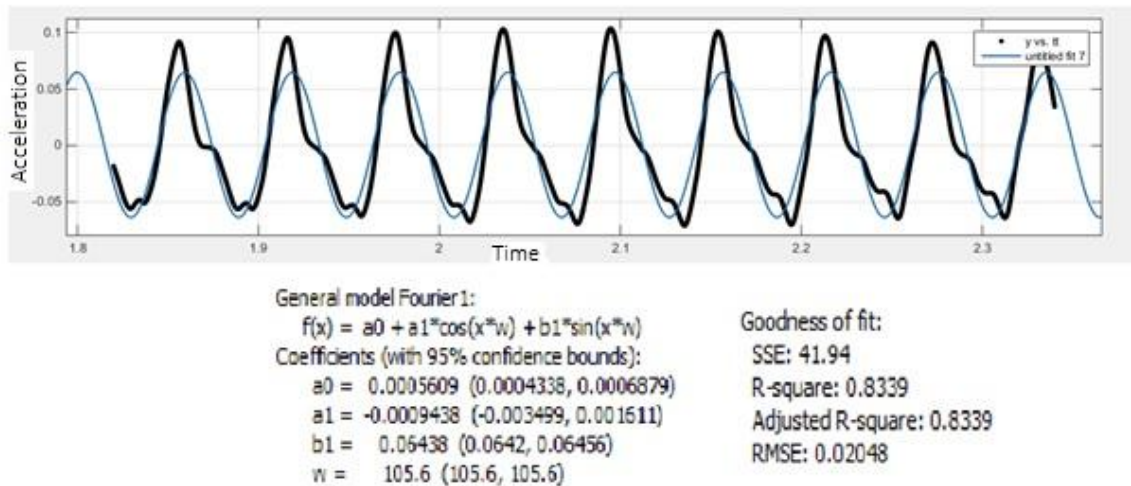


Fig. 412 - Approximation of filtered signal of acceleration and model of acceleration.

#### 4.4.4 Measurement and design conclusions

From the whole work with the exciter it is obvious that the construction of the exciter and the hoist must be well managed. Primarily their connection because the hoist sometimes “jumped off”.

From the experiment data it is obvious (pictures 410, 411 and 412 show the most typical result) that the model doesn't capture the full mechanical properties. The motion of the mass  $m$  sometimes experiences imperfections in oscillation and the motion is not harmonic. That is proven by the shape of the signal in picture 412 or by the large number of peaks in DFT around the examined frequency in picture 410. This doesn't have to be just noise. These imperfections as well as the jumping off of the hoist are probably caused by bad connection between the eccentric and the hoist.

The imperfections in oscillations that are mentioned above can also arise from instability of drive operation. This instability can be caused either by the character of drive load or probably by wrong choice of a drive and its operation. This drive was used because it was available, and it was needed only for short experimental time. But it showed that choosing good drive is a really important aspect of modal analysis and it needs to be investigated further.



## **4.5 Experiment summary**

Based on the findings in this chapter it is clear that the model of the system must be appropriately expanded up to the level of the drive. Furthermore, the construction needs to be examined more thoroughly and the connection between the hoist and the eccentric needs to be perfected (more research needs to be done regarding the normal force) and also to resolve the properties of the drive. This will be addressed in the next chapter.

## 5. Optimization

At first, we need to create a model which will capture all of the previously neglected dynamics. From this model we can then follow with all of our designs and ideas. This model is in the picture 501. Later it will be slightly simplified nevertheless it will still capture reality better than model in previous chapter. There is considered the mass of the hoist ( $m_2$ ), normal force between the hoist and the eccentric and also the properties of the drive and elements directly or indirectly attached to it. The analysis of the whole model will be discussed later.

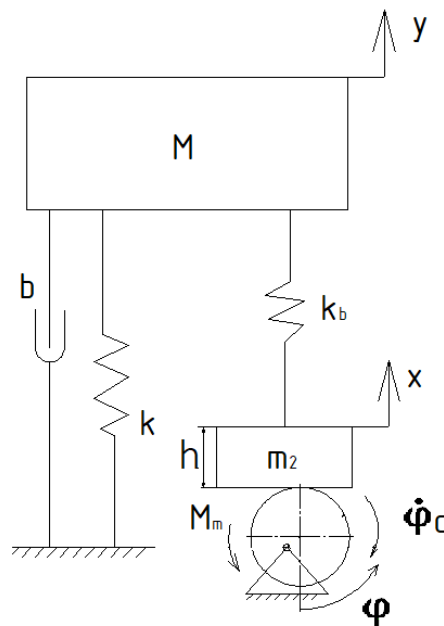


Fig. 501 – Sketch of full model

In the first part of optimization we will address the problem of increasing exciting force with increasing frequency and rebound of hoist. We will try to solve this by setting mechanical parameters for **each tested frequency**.

In the next part we will look at the complete model.

### 5.1 Optimization of mechanics

In picture 501 is diagram of complete model in terms of physics of the mechanical exciter. But this model is unnecessarily complicated and would cause only problems in optimization computations as it would increase the computation time.

## 5.1.1 Model for optimization

For the following calculations we will take away the eccentric with the drive. Mass  $m_2$  will be then thought of as harmonically moving at a constant frequency and we will keep the normal force  $N$ . This harmonic motion should have been ideally excited by the eccentric.

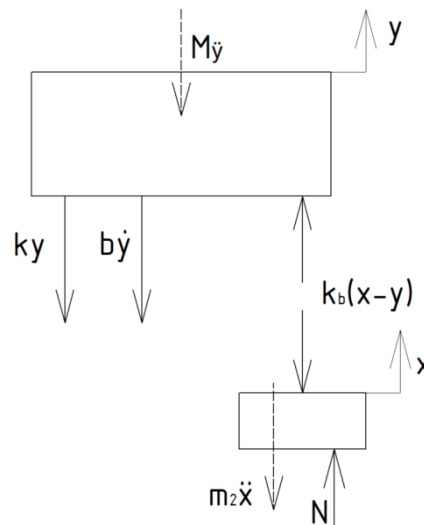


Fig. 502 – Free-body of the modified system

In Picture 502 is shown the modified model as was described before and its Freebody. From the dynamic Free-body we can assemble equations for mass  $M$  and  $m_2$ :

$$M\ddot{y} + b\dot{y} + k_b(x - y) + ky = 0 \quad (5.1)$$

Where  $M$  is the sum of the mass of the table  $m_0$  and mass of the excited system  $m$ ,  $b$  is the dampening coefficient and  $k_b$  is the stiffness of the spring through which is transferred the excitation of mass  $m_2$  on mass  $M$ .

$$m_2\ddot{x} + k_b(x - y) - N = 0 \quad (5.2)$$

Where  $m_2$  is the mass of the hoist.

If we substitute mass  $m_2$  for the harmonic motion  $x$ :

$$x = e * \sin(\omega t) \quad (5.3)$$

And acceleration:

$$\ddot{x} = -\omega^2 e * \sin(\omega t) \quad (5.4)$$

Then we will get from equation 5.1 and equation:

$$M\ddot{y} + b\dot{y} + (k_b + k)y = k_b * e * \cos(\omega t) \quad (5.5)$$

And from equation 5.2:

$$-\omega^2 e * \sin(\omega t) * m_2 + k_b(e * \sin(\omega t) - y) = N \quad (5.6)$$

This model is good but in reality, the spring  $k_b$  will be predeformed because of design and so we need to add this predeformation into the equation. Let this predeformation be  $r_0$ .

On the equation describing the oscillation of mass  $M$  this predeformation will affect only the static equilibrium point. This shift in the equilibrium will be derived later. On the equation describing the motion of  $m_2$  the predeformation will have a direct effect because the reaction force between the eccentric and hoist is added to it. Therefore, the preload must be added to the term describing the force on the spring of stiffness  $k_b$ . The equation 5.6 will then look like:

$$-\omega^2 e * \sin(\omega t) * m_2 + k_b(e * \sin(\omega t) - y + r_0) = N \quad (5.7)$$

### 5.1.2 Equilibrium point

It is important to keep in mind that the predeformation in the spring is caused by the displacement of the eccentric (in pic.403 the change of the distance  $u$ ) but this change is not caused by the predeformation of the spring! This predeformation must be calculated from equilibrium of forces 5.8.

$$g * (M + m_2) + k * (y_0 + l_0) + k_b * (y_0 - [a_0 + u]) = 0 \quad (5.8)$$

Where  $l_0$  and  $a_0$  are free lengths of the springs  $k$  and  $k_b$ .

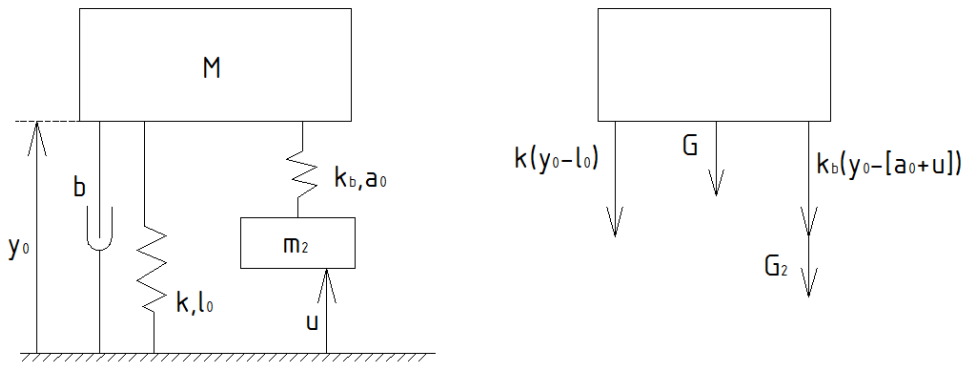


**Fig. 503 - Equilibrium point and its free-body**

From equation 5.8 can be expressed:

$$y_0 = \frac{k \cdot l_0 + k_b \cdot (a_0 + u) - g \cdot (M + m_2)}{k + k_b} \quad (5.9)$$

And finally the predeformation of the spring  $r_0$  is given by the equation:

$$r_0 = y_0 - [a_0 + u] \quad (5.10)$$

This is the equation from which we will determine the change in height position of the eccentric in order to satisfy the  $y_0 - [a_0 + u]$ .

### 5.1.3 Optimization parameters

As it's described above the excitation force in this type of exciter is created by the inertial force of the table and the attached system. The downside is that the excitation force increases with the frequency because the acceleration on mass increases. In the optimization we will focus on choosing the right parameters to alter the behavior of the shaker. These parameters will then be optimized so that we get desired behavior at each frequency. Such parameters will then be used for setting the device.

If we look at equations 5.5 and 5.7 we see that in theory, we can manipulate with these parameters:

- 1)  $k$  ... main stiffness
- 2)  $M$  ... mass of the object
- 3)  $k_b$  ... stiffness over which the excitation is done
- 4)  $e$  ... eccentricity
- 5)  $r_0$  ... predeformation
- 6)  $m_2$  ... mass of the hoist

These are all the “free constants” that can be manipulated in some way (except for dampening). When we look at  $M$  we find out that it is in fact the sum of the mass of the table  $m_0$  (the mounting) and mass of the tested system  $m$ . So, the only parameter that can be changed is the mass of the table  $m_0$ .

With parameters  $e$  and  $r_0$  there are no bigger problems. We only need to keep in mind that they need to be in feasible range. In reality their setting can be done with proper construction so that the eccentricity could be changed with actuator  $a$  so the predeformation of a spring  $k_b$  could be changed either by changing the position of a shaft of the eccentric or directly on the spring  $k_b$  (air spring). Mass  $m_2$  will be probably small and will have only small impact. Therefore, it will not be used as an optimization parameter.

With the stiffness  $k$  and  $k_b$ , we need to realize that (along with parameter  $M$ ) they have impact on the natural frequency of the system and that is why we need minimal stiffness. Parameters of these springs can be adjusted either by construction or using the air springs.

On the other side are parameters for objective function. In this case these are:

- 1)  $\ddot{y}$  ... acceleration of mass  $M$
- 2)  $y$  ... displacement of mass  $M$
- 3)  $N$  ... normal force between  $m_2$  and eccentric

With the acceleration  $\ddot{y}$  it is obvious that it needs to be constant for all frequencies and have the required value corresponding to the exciting force.

The displacement of the mass is not so important. It only needs to be checked. Even though we will keep it as an optimized parameter with small importance.

With normal force it is more complicated. This force should not change “the sign” because of rebound (even though this problem can be solved with construction method). That is why its minimal value should be positive. (This condition is beneficial in terms of load as well). It is also important to keep track of its maximal value because of the overall strength of the system and the requirements of the drive.

#### **5.1.4 Mathematical optimization**

When we look at optimization parameters and think about the real construction then it is obvious that not all of them will be possible to quickly and easily change between different frequencies. These parameters are namely  $m_0$  and  $k$ . With the mass of the table it goes without saying that it should be constant and changing its mass would be complicated.

Also, having all springs to be air springs seems to be ineffective. That is why we decided to divide this problem into two optimizing tasks.

In the first one will be optimized all five parameters ( $k$ ,  $m_0$ ,  $k_b$ ,  $e$ ,  $r_0$ ) and according to the results will be chosen values for  $k$  and  $m_0$ . These will be used for construction and later for the second optimization.

In the second optimization will be only three parameters for optimization ( $k_b$ ,  $r_0$ ,  $e$ ) that has been already optimized in the first optimization. The results of this optimization will be used for construction and later setting the shaker for modal test.

#### ***Objective function***

The objective function will be made for the optimization algorithm. The objective function will be the same for both optimizations. As was mentioned earlier the parameters for the objective function are acceleration  $\ddot{y}$ , position and the range of the normal force. For each of these elements is necessary to implement criteria individually.

#### **Normal force**

For the normal force we have two conditions. It mustn't go over certain maximal value and it mustn't be negative; respectively it mustn't go under certain value (the normal force mustn't be negative in order to prevent jumping off).

At first look it seems that for the objective function these problems are identical. However, during calculation it turned out that regarding the maximum of the normal force it is better to keep it at maximum. The optimization then converged to better results. For the objective function the maximal normal force is given by equation:

$$CF1 = (N_d - \max(N))^2 \quad (5.11)$$

Where:

$N_d$  ... maximal allowed normal force

$\max(N)$  ... maximal normal force

The requirement on the maximal force is solved by the penalization condition. If the minimal force is less than the required value the objective function will add a large number to the result. If the force is greater nothing will happen.

Position

For the position (maximal displacement) isn't the condition very important but we will still set it as a requirement to keep a certain maximal displacement. The solution is then analogical to the setting of the maximal force. The objective function CF2 for maximal displacement is then going to be given by the equation:

$$CF2 = (y_d - \max(y))^2 \quad (5.12)$$

Where:

$y_d$  ... required displacement

$\max(y)$  ... maximal displacement

Acceleration

For acceleration the situation is really simple. Acceleration needs to be set as constant. Therefore, the objective function will be given by equation:

$$CF3 = (\ddot{y}_d - \max(\ddot{y}))^2 \quad (5.13)$$

Where:

$\ddot{y}_d$  ... required value of acceleration on mass M

$\max(\ddot{y})$  ... maximal acceleration on mass M



And the final objective function is:

$$CF = I_1 * CF1 + I_2 * CF2 + I_3 * CF3 + \textit{penalization}$$

(5.14)

Where:

$I_i$  ... significance for each individual part of the objective function  
penalization ...value added to the result if the normal force falls below the set value

With the masses it's important to keep in mind that they need to be normalized or they need to be set with multiple optimizations using the method try-and-see.

This objective function will be minimized for each tested frequency. From this will be determined the optimal parameters. With these parameters the system will operate in required values.

### ***Parameter guess***

For the optimization it is necessary to at least crudely guess the parameters values for the program to use as starting points. It is obvious that they will depend on the physical properties and the construction of the system.

It turns out that subresonance execution of the shaker is better for smaller masses and smaller accelerations. This is clearly demonstrated by the experiment. Although the model did not quite match the theory and the oscillation wasn't harmonic (problem in construction) the shaker still worked and was able to make the matter move.

For larger values of mass and acceleration the stiffness  $k$  would have to be much larger (in orders of  $10^7$  N/m) and that caused large force acting on the frame and the drive. Theoretically it can't be considered not feasible but practical execution would be too complicated.

It was decided with my supervisor that we will abandon the values used for the model (we will increase the significantly) and further work will be done in more common suprapresonance build.

Parameters for following calculations are:

- Maximal acceleration on excited system is 10 m/s<sup>2</sup>
- Maximal mass of excited system is 50 kg
- Frequency range 5 to 50 Hz

For calculations will be used maximal (or minimal) values because it can be expected they will generate the greatest load and the most complicated situations.

### Dampening b

This parameter is not part of the optimized parameters. Nevertheless, it cannot be forgotten because it will speed up when the homogenous solution of differential equation 5.5 reaches zero. Characteristic equation for this differential equation of second order will be (solved according to [pg. 23 13]):

$$\lambda^2 + \frac{b}{M}\lambda + \frac{(k_b+k)}{M} = 0 \quad (5.15)$$

Where the solution of this equation can be rewritten as:

$$\lambda_{12} = \frac{-\frac{b}{M} \pm \sqrt{\left(\frac{b}{M}\right)^2 - 4\frac{(k_b+k)}{M}}}{2} \quad (5.16)$$

Assuming that b/M, although squared, will be definitely smaller then second term under the square root, the solution can be expected in form:

$$\lambda_{12} = -\frac{b}{2M} \pm i \frac{\sqrt{\left|\left(\frac{b}{M}\right)^2 - 4\frac{(k_b+k)}{M}\right|}}{2} \quad (5.17)$$

And from that can be derived a homogenous solution of differential equation:

$$y_h = C_1 * e^{-t\frac{b}{2M}} * \cos\left(\frac{\sqrt{\left|\left(\frac{b}{M}\right)^2 - 4\frac{(k_b+k)}{M}\right|}}{2}\right) + C_2 * e^{-t\frac{b}{2M}} * \sin\left(\frac{\sqrt{\left|\left(\frac{b}{M}\right)^2 - 4\frac{(k_b+k)}{M}\right|}}{2}\right) \quad (5.18)$$

In the equation 5.18 can be seen two exponentials which determine the fading of the homogenous solution (reaching zero). This can be expressed as:

$$e^{-t\frac{1}{\tau}} = e^{-t\frac{b}{2M}} \quad (5.19)$$

Where  $\tau$  is time constant of the exponential:

$$\tau = \frac{2M}{b} \quad (5.20)$$

And the time of fading of the homogenous solution (time needed to fall for 98% of the value) can be calculated as:

$$t_s = 5\tau = 10 \frac{M}{b} \quad (5.21)$$

All this will be of course affected by the start-up of the drive, control of the drive, etc. Nonetheless this needs to be taken care of. For the following calculation we will assume dampening  $b=10$  Ns/m, which corresponds to  $t_s=50$  s. In reality I would expected the time to be shorter, given the reasons mentioned before and experiences from practical experiments. The final choice of dampening will depend on the final behavior of the system. The advantage is direct proportion between the time of stabilization and the mass of the system – with lower load it will stabilize faster.

Stiffness  $k$ :

This stiffness needs to be limited at its maximal value. This comes from the need to have the natural frequency lower than the lowest operation frequency. The natural frequency of mass oscillation on a spring can be calculated from:

$$\omega_n = \sqrt{\frac{K}{m_s}} \quad (5.22)$$

Where:

$K$  ... Stiffness of the spring

$m_s$  ... Mass of the oscillating object

When we look at our system it is obvious that mass  $M$  is oscillating on spring  $k$ .

Let's substitute terms in equation 5.22:

$$\omega_n = \sqrt{\frac{k}{M}} \quad (5.23)$$

From this we can express k and substitute  $\omega_n$  for frequency in Hertz:

$$k = (2\pi f_n)^2 * M \quad (5.24)$$

When we consider that the table will have some mass of its own and the system will be attached to it then we can guess the minimal mass M to be approx. 5 kg. Next, giving us some “wiggles room” from the minimal operation frequency then we can set  $f_n$  to be 4 Hz. When we do the calculation for 5.24 we get:

$$k = (2\pi * 4)^2 * 5 = 3157 \frac{N}{m} \quad (5.25)$$

The stiffness should not exceed approximately 3000 N/m.

Stiffness  $k_b$ :

This stiffness is linked to the mass  $m_2$ . This mass is expected to be small. From the construction point of view, it means part of the mass of the eccentric, its housing and spring connections (let's say 2 kg). During the calculations it turned out that this stiffness needs to be larger. That's why it is better to move the natural frequency of this subsystems shift to the area above operation frequency. Leaving some reserve again let's assume that the natural frequency should be approx. 70 Hz. We can plug the numbers in like previously to the equation 5.24 and we are getting:

$$k_b = (2\pi * 70)^2 * 2 = 3,9 * 10^5 \frac{N}{m} \quad (5.26)$$

Stiffness  $k_b$  should not go lower than  $4 \times 10^5$  N/m.

Weight  $m_0$

This mass is closely linked to the stiffness k and it's mentioned there. Its value doesn't have an upper limit and theoretically neither lower limit. Practically, the table can't have zero mass. And with large mass the mass options of the system would be limited. As the guess for the calculation we shall use  $m_0=2,5$  kg.

Eccentricity  $e$  and preload  $r_0$

These constants are linked together. And they are also linked to the stiffness  $k_b$  and the normal force. Here we really did not care about scientific guesses and left values of  $e$  to be from the interval  $\langle 0;10 \rangle$  mm and  $r_0$  from the interval  $\langle 0;15 \rangle$  mm while we set the initial guesses to be 1 mm and 5 mm.

With all these parameters it's important to note that they are only guesses. If it were to come to design, it would have to be modified for given situation. Here we are trying to come up with parameters for very universal device. This device could theoretically work with quite large range of masses, frequencies and accelerations (corresponding to the exciting force).

### ***The optimization***

Now we will show the inputs and outputs of both optimizations described above. The result will be parameters for design and settings of the shaker for modal analysis. Optimization will be done with function FMINCON. On the web pages of MathWorks are no details on this function so here is a brief description according to [15]:

Function FMINCON finds the smallest solution to a given function. It uses nonlinear programming method and it can move between different methods during calculation. This solution can be either scalar, vector or a matrix. The function will search for solution from a certain starting value that is given by the user. The user can also constrain what the solution is supposed to look like. In that case the FMINCON will not return the global minimum of the function (assuming it has one) but only a value that is as close to the smallest value as the constrain allows. The given function can be any multivariable constrained nonlinear function. Additional information's are available on the web pages at [15].

## Optimization of the five parameters

Initial guesses of optimized parameters:

- $m_0 = 2.5$  kg
- $r_0 = 5$  mm
- $e = 1$  mm
- $k = 3000$  N/m
- $k_b = 4.5 \times 10^5$  N/m

Parameters of the objective function:

- Maximal N = 1000 N
- Minimal N = 10 N
- Acceleration  $\ddot{y}$  = 10  $\text{m/s}^2$
- Displacement  $y = 2$  mm

Solution:

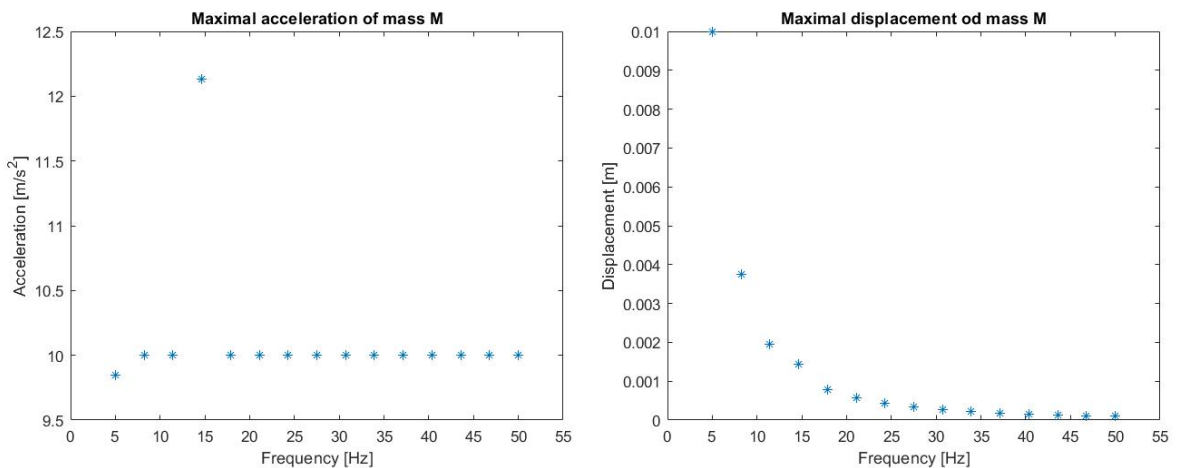


**Fig. 504 - Graphs of acceleration and displacement**

In picture 504 can be seen that acceleration is stable with occasional deviation. That is probably caused by the local optimization method. Displacement gradually decreases and except for the first value is it nowise high.

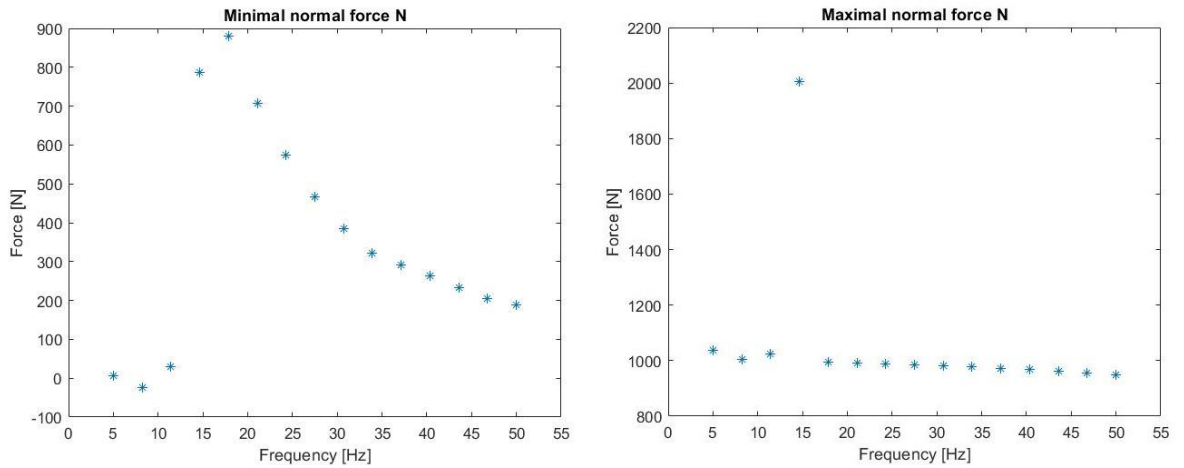


**Fig. 505 – Graphs of minimal and maximal normal force**

On picture 505 can be seen minimal and maximal normal force. Minimal force in some parts slightly decreases less than zero but that is not relevant. This optimization is used to approximate some parameters. In principle, the maximal force holds the required value with occasional deviation, same as acceleration.

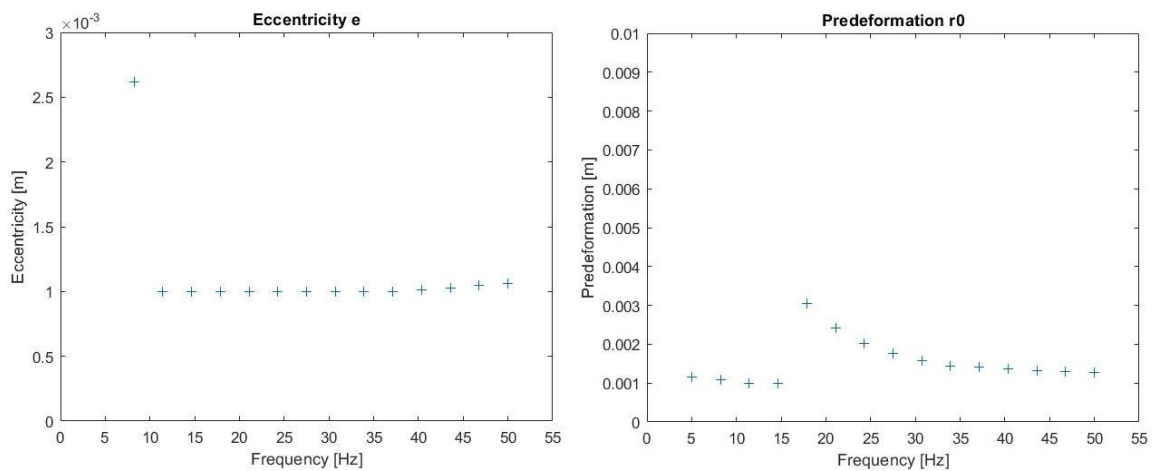


**Fig. 506 – Graphs of eccentricity and predeformation**

Picture 506 shows values for eccentricity and predeformation. These values are not that much interesting. All the values are within reasonable boundaries.

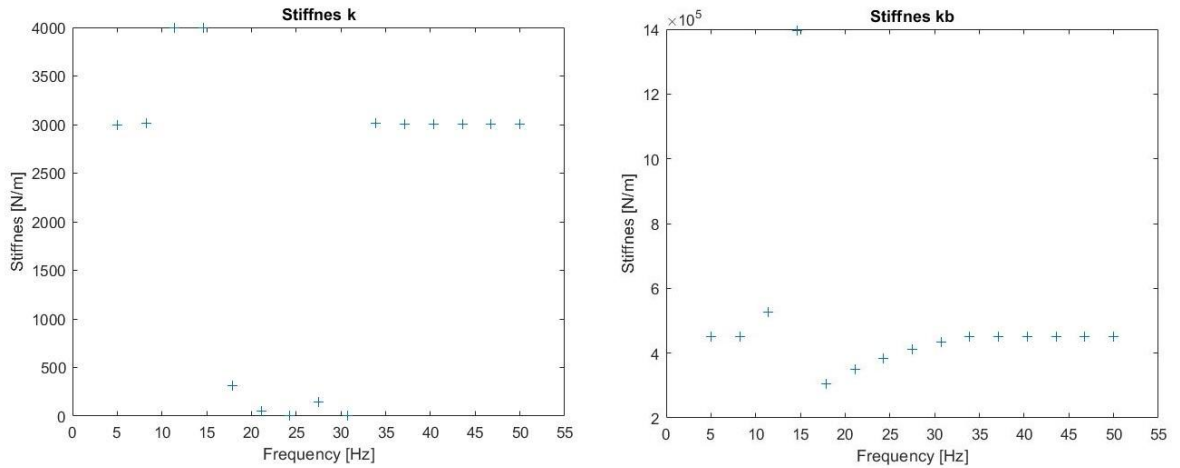


**Fig. 507 – Graphs of stiffness  $k$  and  $k_b$**

Picture 507 shows the value of stiffness  $k$  and  $k_b$ . Both values have the trend to decrease. With  $k$  value, it is no obstacle so for the next optimization that value will be decreased. With spring  $k_b$ , it is an obstacle so for the next optimizations the lower limit for  $k_b$  rigidity will be set.

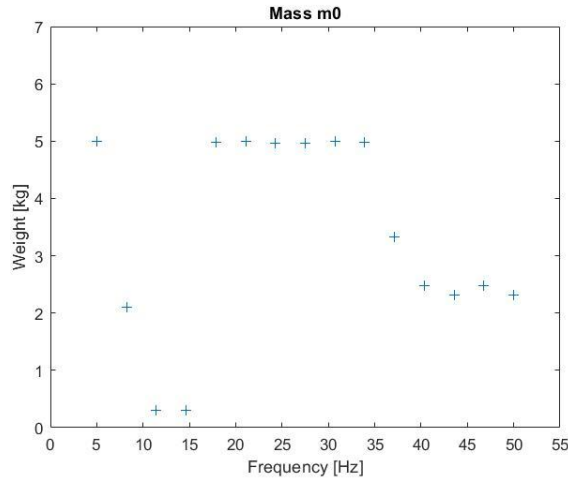


**Fig. 508 – Graph of weight of table**

From the picture 508 is evident that weight  $m_0$  has trend to be higher and is stopped by the maximal allowed weight (within optimization). So, for the next steps that value will be increased.



Output:

- $m_0 = 3$  kg
- $k = 2500$  N/m

Settings for the lower limit of stiffness  $k_b$  at  $4 \times 10^5$  N/m.

### Optimization of the three parameters

Inputs for this optimization remain the same as for previous optimizations. Only the quantity of optimization parameters will change and  $k$  and  $m_0$  will be set base on previous optimization outputs.

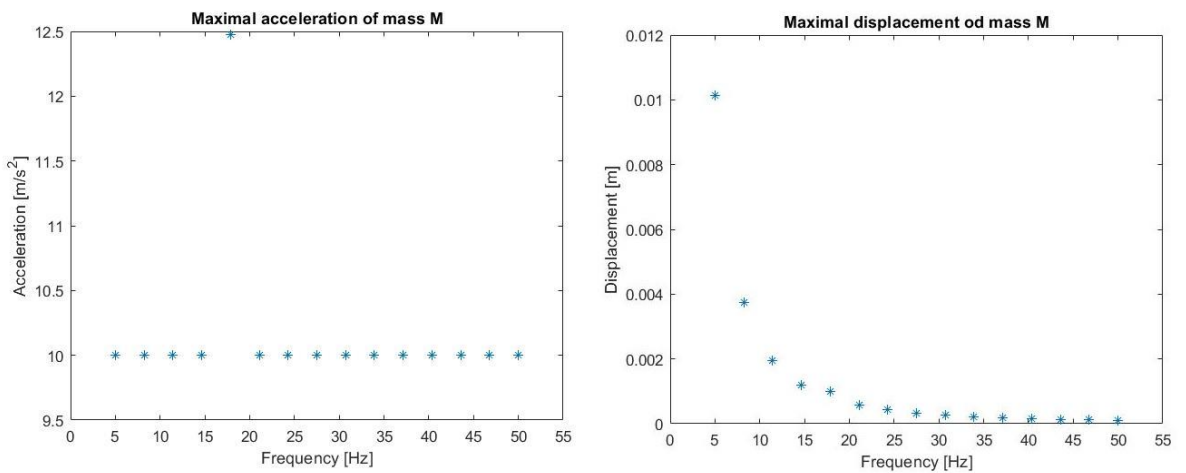


**Fig. 509 –Graphs of acceleration and displacement**

On picture 509 is a graph for acceleration and weight M displacement. Values for acceleration are on demanded base with one exception. This problem is almost certainly caused by optimization which found the different local minimum. This problem could be solved by the manual change of eccentricity or predeformation. Deviation itself is in acceptable limits (without first value). That can be solved by lowering requirements on acceleration or stiffness  $k$ .

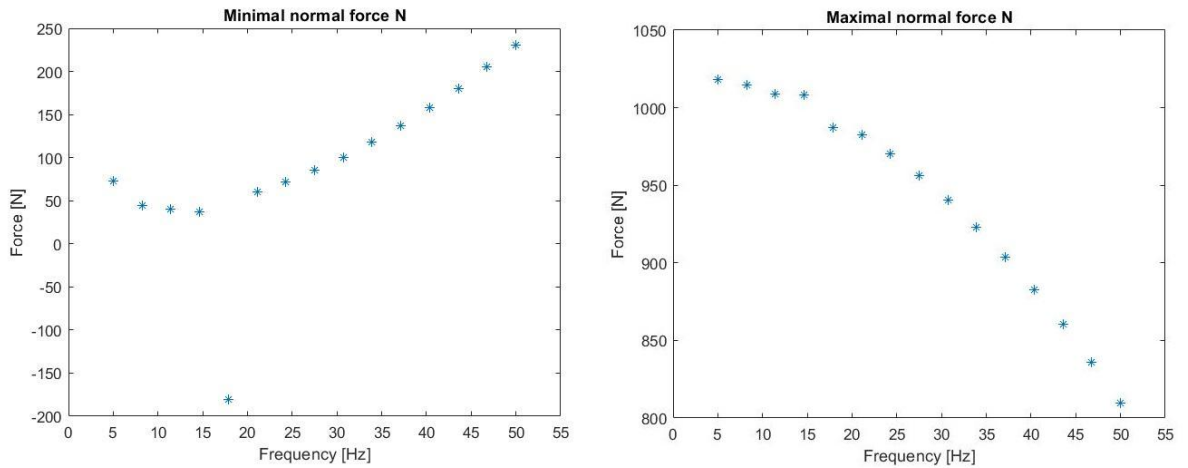


**Fig. 510 – Graphs of minimal and maximal normal force**

Picture 510 shows the graph with minimal and maximal normal force. Minimal force is within positive required limits within one exception. This exception is on the same frequency as on the previous graph, which can be excepted. Reason and solution could be the same. Maximal normal force did not exceed limits that much and gradually decreases which is good.

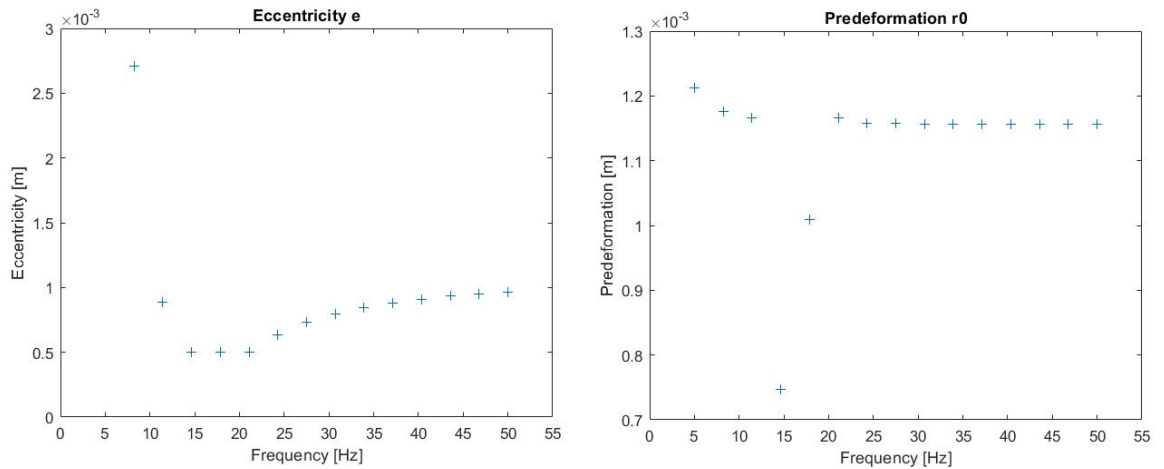


**Fig. 511 - Graphs of eccentricity and predeformation**

Picture 511 shows graphs of eccentricity and predeformation. Both parameters are within required limits. However, it shows that with constant stiffness  $k$  the eccentricity influence is more visible. With stiffness  $k$  changes influence of bias was more significant and eccentricity influence was smaller.

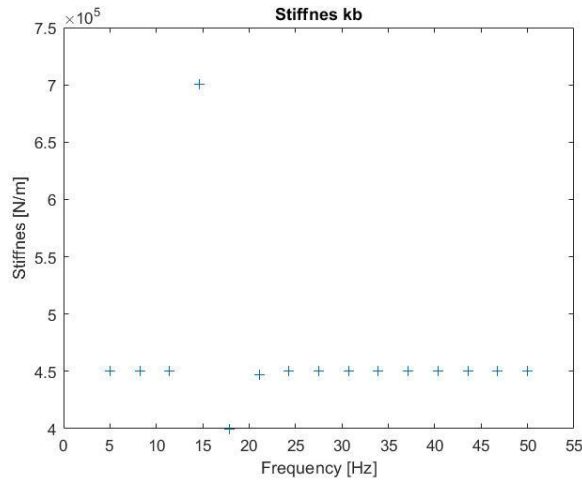


**Fig. 512 – Graph of stiffness  $k_b$**

Picture 512 shows stiffness values  $k_b$ . They are relatively stable. Change of  $k_b$  stiffness is useful with acceleration changes not with frequencies changes.

### **Summary**

After performing the calculations, it turns out that this approach is functional. At least for one chosen mass and acceleration everything can be set so that the device works as it should.

Of course, more calculations were done than is documented here in this thesis. Experience from this calculation tells us that it is useful to manipulate with the setting of the maximal normal force in the objective function and that in the middle of the frequency range it is useful to allow decrease in stiffness  $k_b$  under the minimal value calculated from equation 5.26 specially when trying to reach lower accelerations. This stiffness is set for the maximal frequency and therefore this stiffness can be lower at lower frequencies. The same applies for smaller masses.

Furthermore, it can be said that the optimization process is reaching its limits but that can be solved by logically interfering with the parameters.

And at last we have to point out that it is better for the optimization to have “free hands” and occasional conflicting regions evaluate one by one.

## 5.2 Complete model

In picture 513 is show the complete model and its Free-body.

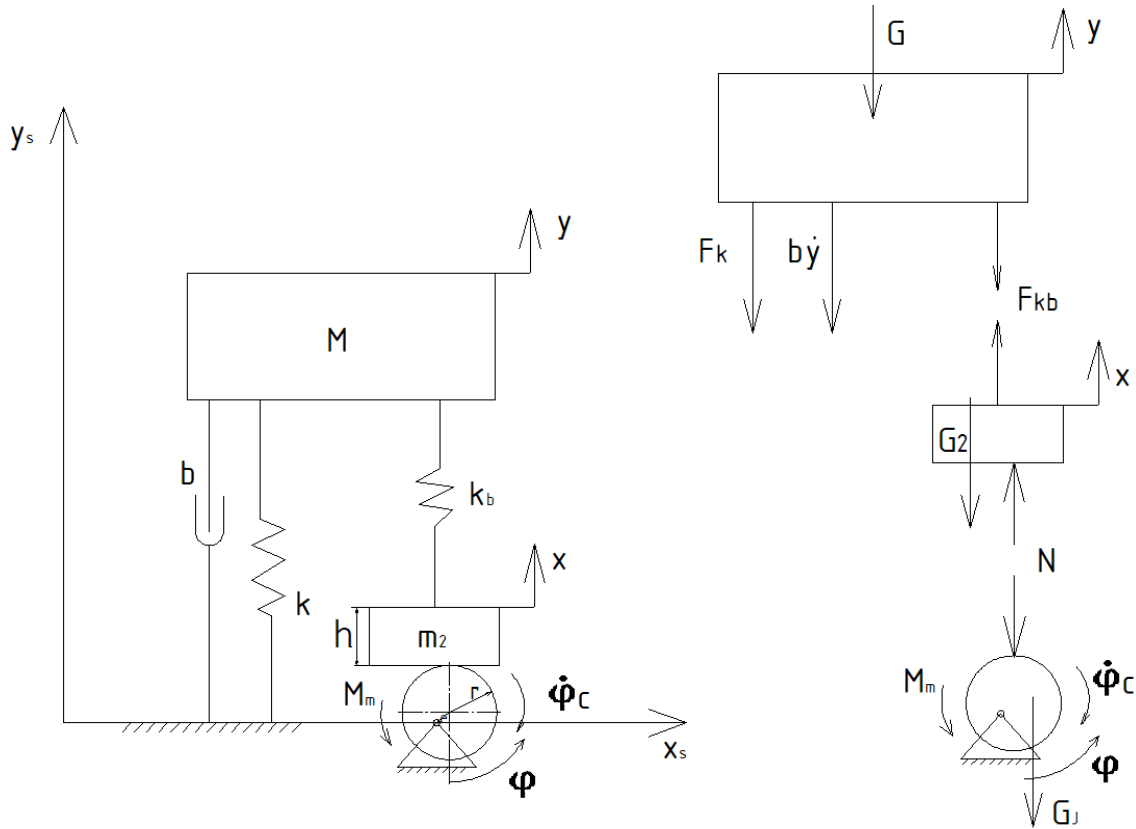


Fig. 513 – Sketch of model and its free-body

According to picture 513 we can derive equations for individual bodies.

Mass  $M$ :

$$M\ddot{y} = -G - F_k - \dot{y}b - F_{kb} \quad (5.27)$$

Mass  $m_2$ :

$$m_2\ddot{x} = N - G_2 + F_{kb} \quad (5.28)$$

Rotating mass  $J$ :

$$J\ddot{\varphi} = -Necos(\varphi) - G_Jecos(\varphi) + M_m - \dot{\varphi}c \quad (5.29)$$

Where  $c$  is the dampening of the rotation.

Now let's substitute the forces in springs and the masses into equations 5.27 and 5.28.

$$M\ddot{y} = -Mg - (y - l_0)k - \dot{y}b - (y - l_{02} - h - x - r_0)k_b \quad (5.30)$$

$$m_2\ddot{x} = N - m_2g - (y - l_{02} - h - x - r_0)k_b \quad (5.31)$$

Where  $l_0$  and  $l_{02}$  are free lengths of springs  $k$  and  $k_b$ .

Furthermore, we know from kinematic relationship for eccentric:

$$x = r + e \sin(\varphi) \quad (5.32)$$

$$\ddot{x} = e \cos(\varphi) \ddot{\varphi} - e \sin(\varphi) \dot{\varphi}^2 \quad (5.33)$$

From equations 5.32 and 5.33 we can substitute to equations 5.30 and 5.31:

$$M\ddot{y} = -Mg - (y - l_0)k - \dot{y}b - (y - l_{02} - h - e \sin(\varphi) - r - r_0)k_b \quad (5.34)$$

$$m_2(e \cos(\varphi) \ddot{\varphi} - e \sin(\varphi) \dot{\varphi}^2) = N - m_2g - (y - l_{02} - h - e \sin(\varphi) - r_0)k_b \quad (5.35)$$

From equation 3.35 we can isolate the force  $N$  and then substituting into equation 5.29 along with substitution for force  $G_j$ :

$$\begin{aligned} \ddot{\varphi}[J + m_2(e \cos(\varphi))^2] = & \quad (5.36) \\ -e \cos(\varphi)[m_j g - m_2 e \sin(\varphi) \dot{\varphi}^2 + m_2 g + (y - l_{02} - h - e \sin(\varphi) - r - r_0)k_b] - \dot{\varphi}c + M_m \end{aligned}$$

Next this model needs to be expanded for the model of the drive which has been so far represented as a term  $M_m$  as a torque from the drive. This torque can be expressed as:

$$M_m = k_m i \quad (5.37)$$

Where  $k_m$  is the constant of the drive and it is the current coming to the armature of the drive.

The equation for the circuit of the armature is:

$$\frac{di}{dt} = \frac{1}{L}(U + Ri + k_m \dot{\phi}) \quad (5.38)$$

Where U is voltage on the armature, R is the resistivity of the armature and L is inductance of the armature.

Now we obtained three differential equations. Two differential equations of second order (5.34 and 5.36) and one of first order (5.38). From these equations we can assemble the state space of the whole system:

$$\dot{x}_1 = x_2 \quad (5.39)$$

$$\dot{x}_2 = \frac{1}{M}[-Mg - (x_1 - l_0)k - x_2 b - (x_1 - l_{02} - h - e \sin(x_3) - r_0)k_b] \quad (5.40)$$

$$\dot{x}_3 = x_4 \quad (5.41)$$

$$\dot{x}_4 = \frac{-e \cos(x_3)[m_1 g - m_2 e \sin(x_3) x_4^2 + m_2 g + (x_1 - l_{02} - h - e \sin(x_3) - r - r_0)k_b] - x_4 c + k_m x_5}{J + m_2 [e \cos(x_3)]^2} \quad (5.42)$$

$$\dot{x}_5 = \frac{1}{L}(U + R x_5 + k_m x_4) \quad (5.43)$$

Where:

- $x_1$  ... displacement  $y$
- $x_2$  ... velocity  $\dot{y}$
- $x_3$  ... angular displacement  $\phi$
- $x_4$  ... angular velocity  $\dot{\phi}$
- $x_5$  ... current  $i$

Unfortunately obtaining parameters for the model of a drive is not easy, the type of drive used in the model is not quite good. There is also not implemented control of the drive. Stabilization of rotations is ensured by adding more dampening  $c$  and more inertial mass  $J$ .

The model was tested at values that came from the optimization for frequency 50 Hz. Given the larger mass  $J$  the angular velocity was stable. The drive operated in the area of its nominal voltage, but in current it was about 50% overloaded.

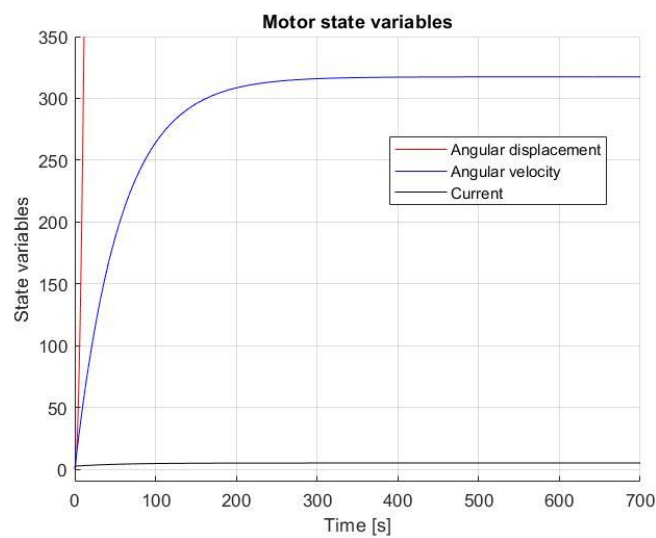
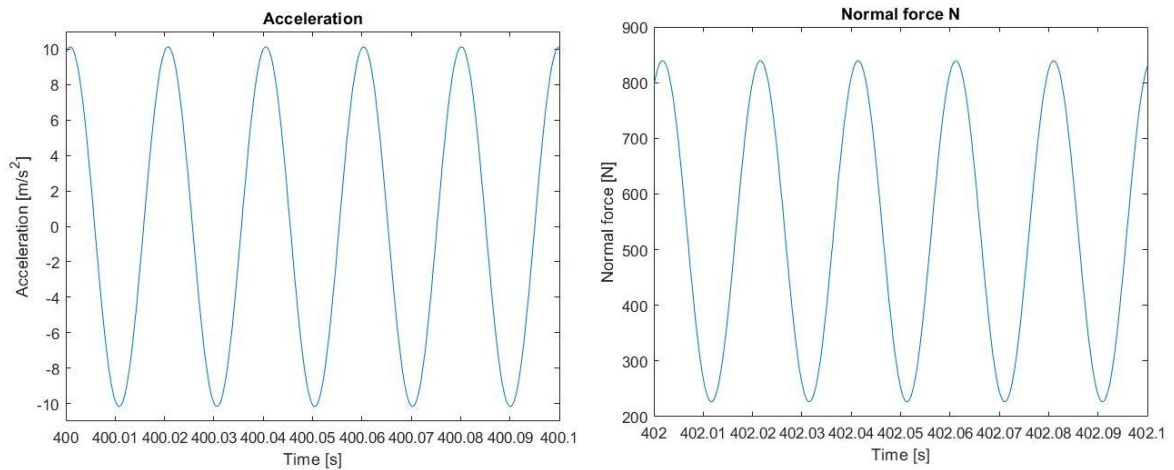


Fig. 514 - Graph of motor state variables

As we can see in picture 513 the angular velocity is stabilized at value corresponding to frequency roughly 50 Hz. The current stabilizes roughly at 5 A which is about twice the maximum value and angular displacement is increasing continuously. The most important parameters for us are acceleration and normal force. These are then compared to optimization in the next part of this chapter.

## 5.2.1 Comparison

The two most important parameters are acceleration on mass M and normal force N.



**Fig. 513 – Graphs of acceleration and normal force 50 Hz**

In picture 513 are time dependencies of these values in equilibrium state for frequency 50 Hz. The values can be compared with graphs in pictures 509 and 510.

When we look at acceleration we can see that its amplitude is slightly higher than the amplitude given by the optimization. The optimization said  $9,995 \text{ m/s}^2$  and the model says  $10,14 \text{ m/s}^2$  for the acceleration.

Certain deviation can be seen even with the normal force. In optimization the normal force was somewhere between 240 and 820 N and during simulation it moved between 230 and 840 N. These deviations were most likely caused by rounding up the parameters  $r_0$  and  $e$  to hundredth of millimeters. This corresponds to the slight increase which can be seen. Another reason for this can be imperfectly set frequency.

The magnitude of the displacement was similar to acceleration. It was also about 1,5% higher. Deviations in the angular velocity were negligible (fractions of rad/s)

That might imply that using smaller inertial mass this deviation might be larger.



Similar comparison was done for frequency 10 Hz. In picture 514 we can see time dependencies of acceleration and normal force in equilibrium state for this frequency.

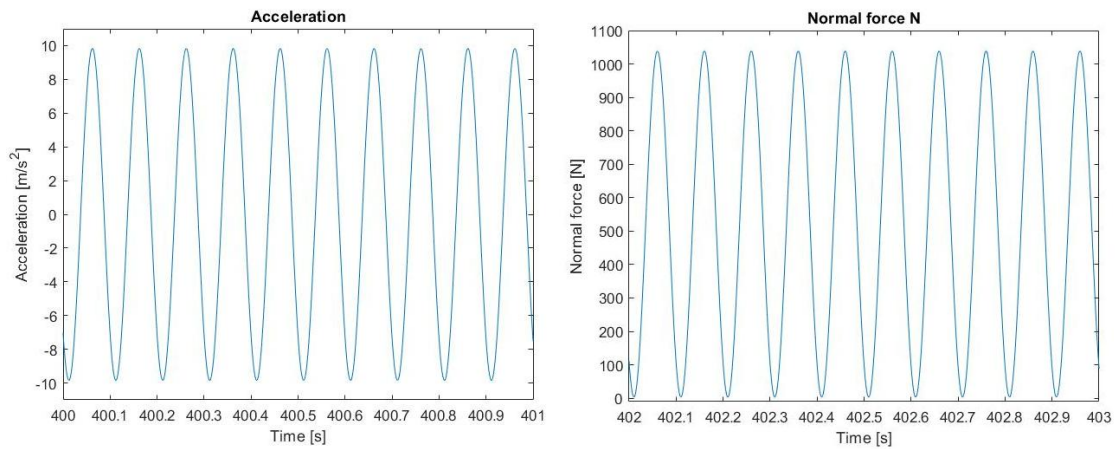


**Fig. 514 – Graphs of acceleration and normal force 10 Hz**

The deviation in acceleration is similarly small as in the previous situation. Optimization stated the acceleration should be  $9,998 \text{ m/s}^2$  and the model gave value  $9,83 \text{ m/s}^2$ . We can see there was small decrease.

For the normal force the values from optimization were between 8 and 1070 N. The model gave values between 4 and 1040 N. We can also see a small decrease.

The parameters  $r_0$  and  $e$  were rounded down to hundredth of millimeters. This corresponds to the slight decrease in the parameters.

In the magnitude of the displacement was observed a decrease just as with the acceleration. The angular velocity as in the previous case deviated in negligible values (again fractions of rad/s) but bit more than in the previous case.

From these statements we can assume that the parameters given by the optimization can be used and the model works as it should.

## 6. Design

The logic of design can be basically the same as with the exciter which is presented in the picture 402 in the previous chapter.

The table is situated on three (possibly more) springs and dampeners. For the subresonance execution these springs will be strongly predeformed with very small stiffness in order to reach sufficient force to balance the weight of the mass  $M$ . To the center of the table will be connected a spring through which will be the table excited.

Throughout the work we were able to identify several important points. First point was the eccentric. It turned out to be problematic right at the beginning of the experiment. It was displaying rebounds and other problems. Also, the biggest load on the system is situated here - the normal force. Another important point were adjustable parameters. The option of setting them asks for a mean how to. With some parameters this solution is purely mechanical - predeformation of the spring  $k_b$ , or as with eccentricity considering multiple options with regard to the acting force. Another problem was the drive. These problems are not visible in the model, but they showed in the experiment. Even though, it is important to keep the problems of the drive in mind.

### 6.1 Eccentric

1)

First solution can be using a cam. But this solution turned out not to be ideal as it is complicated in design. Designing a cam is also hard because the calculations are complicated (for example it is important to calculate the contact pressures) and finding the right material is also not easy. Another downside is that the cam needs to be sufficiently lubricated and it can rebound.

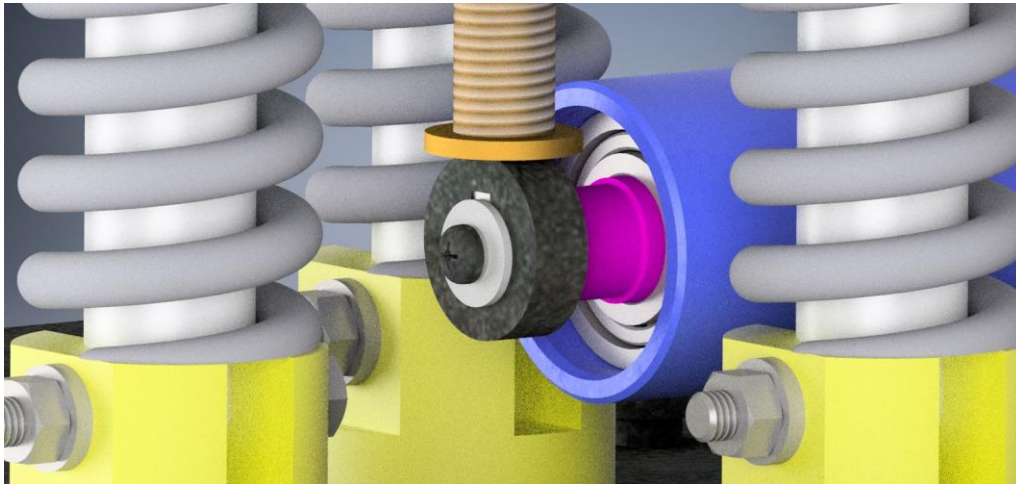


**Fig. 601 – Eccentric cam**

2)

Another option, which was used for the experimental construction, is fitting the bearing on an eccentric plate. There is no problem with calculating the contact pressure as they can be solved by calculating the bearing where contact pressures are already solved by the bearing balls. Nonetheless this does not solve the problem with rebound. This solution is in picture 404 on the left.

3)

The best solution seems to be the design in picture 602. At an eccentrically rotating shaft is a bearing. The bearing is in a housing to which is firmly connected the spring  $k_b$ . The bearing is then moving with the housing and the shaft. Given that the bearing can slip there is no problem with friction. Also, the forces there are known and so the bearing can be easily designed. There is no need for calculating the contact pressures as they are solved by the bearing. The firm connection will also allow for a negative normal force  $N$ . But still it is better to keep the normal force positive (because of for example dilations, load on the bearing, etc.....)

The housing should be attached to something to guide it so that it would not be moving to sides.

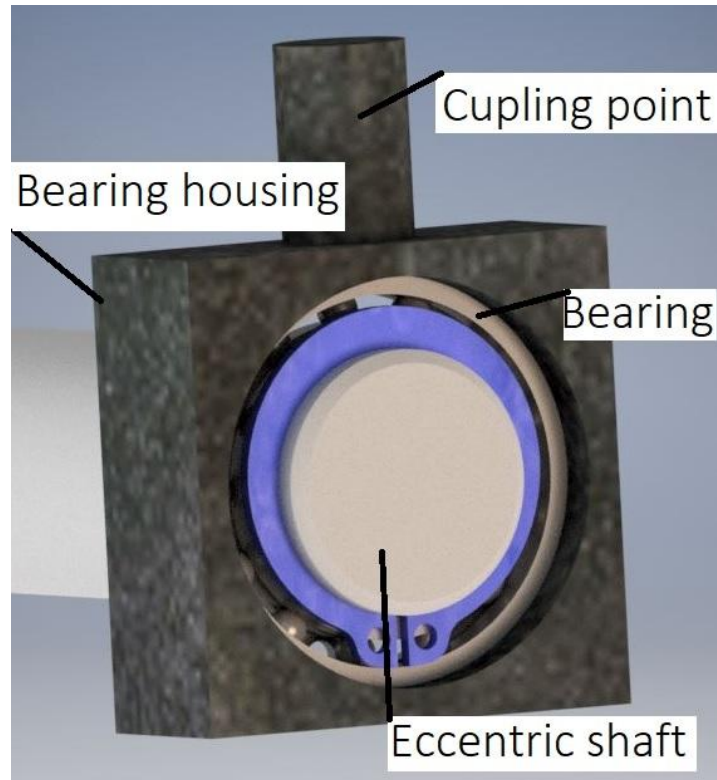


**Fig. 602 – Eccentric with bearing housing**

## 6.2 Adjustable parameters

### 6.2.1 Adjustable stiffness $k_b$

For this stiffness the most obvious and simplest solution is using air springs. It could be said that air spring has significant nonlinear characteristics but that is not an obstacle given that the deviations will be small, and the stiffness can be considered linear in the given operation area. Examples of how such air spring can look like are in picture 603.



Fig. 603 – Air spring [17]

Air springs are commonly used in the industry in large variety of applications. That is why there are many types and sizes of them. For the constructor it surely won't be a problem to choose or design an appropriate spring.

## 6.2.2 Predeformation $r_0$

Solving this is also not a big construction problem. If we go back to the proposal from chapter 4 in pictures 402 and 503 then we can see that we need to move the whole shaft, at which the eccentric is located, for “u”.

Such movements can be achieved by using various actuators (hydraulic, linear servo drives, pneumatic, etc.....). But the situation is then complicated by the connection of the drive if we are not planning on lifting the whole motor.

1)

One of the solutions might be using angular transmission (cardan shaft). The diagram is in picture 604.

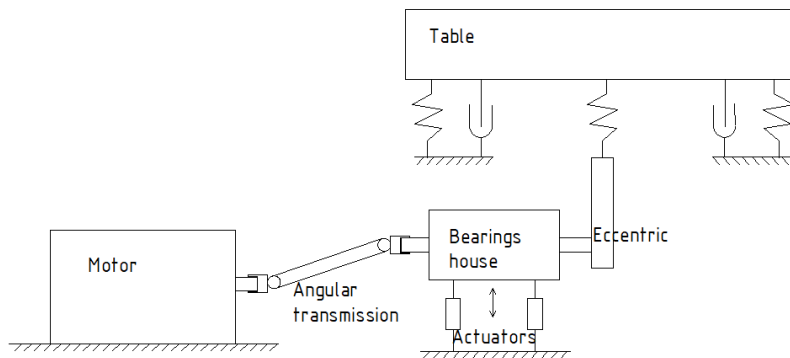
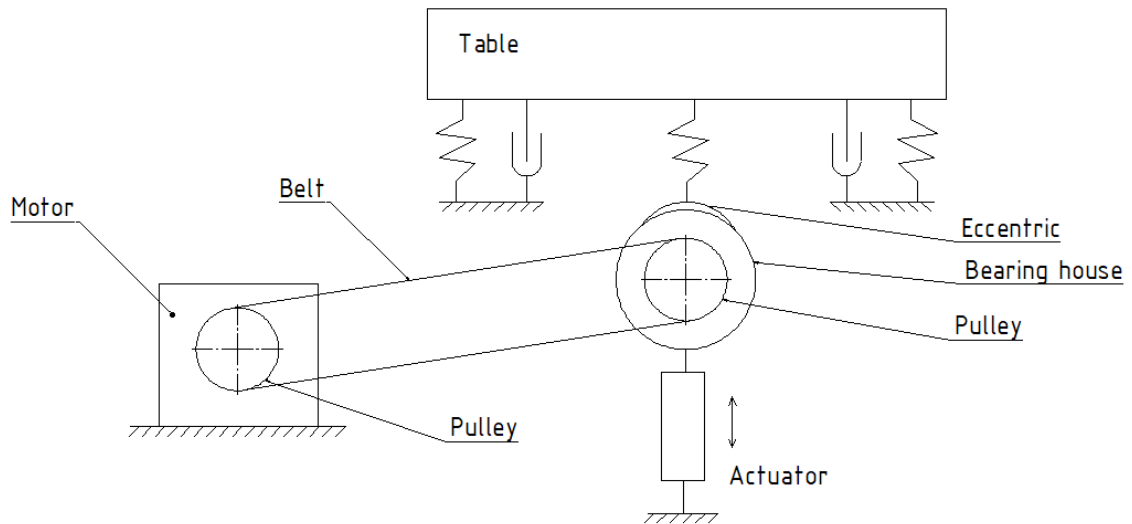


**Fig. 604 – Illustration of concept with angular transmission**

The downside of this design is lower effectively with energy transfer and maybe a bit higher cost. The upside is that these transmissions are stock merchandise and require almost no designing or calculations.

2)

Another option is not connecting the drive directly but through some kind of transmission. In this case the best solution seems to be belt (cog belt). Sufficient length of the belt allows for quite large range of motion of the eccentric's shaft. The diagram



of such set up is in the picture 605.

Fig. 605 – Illustration of concept with belt transmission

The downside might be imperfect transmission of rotations and possibly uneven rotations which can be caused by some means of transmission.

On the other hand, this is quite simple solution which will lower the load on the lifting actuator, allow for higher rotations and can even act as a safety feature – protection from drive overload.

### 6.2.3 Eccentricity $e$

1)

First solution we came up with was to place a linear actuator directly onto the shaft and connect the actuator to the eccentric. Moving the actuator would cause movements of the eccentric from the axis and back and that would change the eccentricity.

This comes with any benefits like changing the eccentricity during operation or possibility for partial balance. For changing the eccentricity there is no need for another device.

But practically this solution is complicated. Common actuators of sufficient size have maximal load tolerance up to 1 kN. Our design of the device operates slightly higher than 1 kN.

Furthermore, it is not ideal to rotate the whole shaft with the actuator.

We believe that an actuator capable of taking the load could be designed but it would be complicated and expensive.

Illustration of such system is in picture 606.

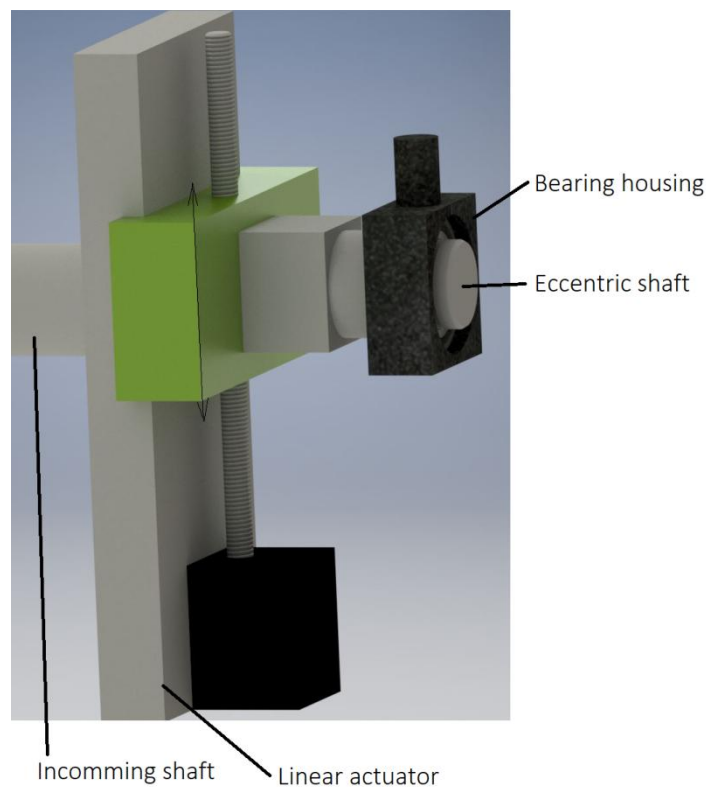


**Fig. 606 – Illustration of concept with linear drive**

2)

Another possible solution, especially for small eccentrics is using double eccentric. This system is used in [4]. The idea is fitting two eccentrics into each other and the eccentricity can be the changed with their relative position.



This solution is simple and inexpensive in terms of construction. The complications come from using actuators for their setting.

Firstly, the system needs to be stopped in a position where the two eccentrics can be released. Secondly, in order to realize the relative positioning of the eccentrics a more complicated actuator is needed.

The main assumption is that the eccentric is supported from one side and allows for the actuator to approach it from next side. The basic concept is in picture 607.

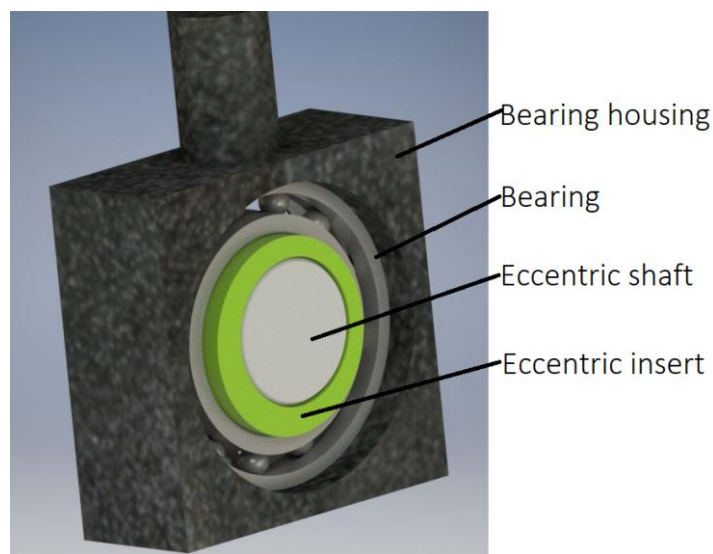


**Fig. 607 – Illustration of concept „eccentric in eccentric“**

The upside of this is then simplicity and cost of the build itself but a certain downside is the complexity of the actuators for setting the eccentricity and the cost of such actuator.

3)

Last proposed design is using crank mechanism. Eccentric is connected by perpendicular screw to the shaft. Angling the screw results in moving the eccentric from the center of the shaft and back which changes the eccentricity. It is similar to the first proposed design. The diagram is in picture 608.

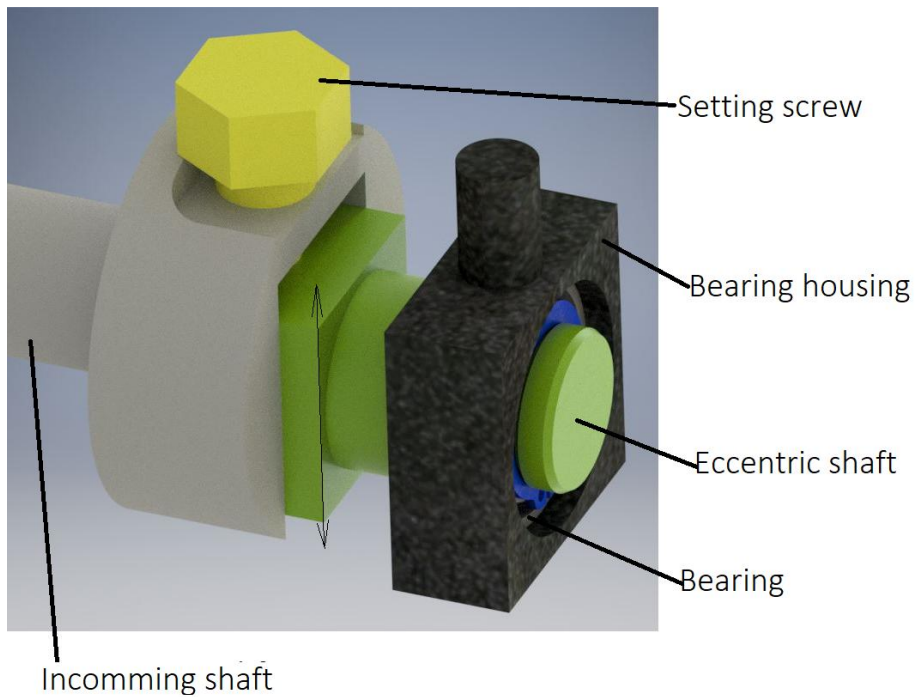


**Fig. 608 – Illustration of concept with setting screw**

From the first design the upside is that the eccentricity can be set during operation. But it does not require any complicated or rotating actuator. For setting the eccentric it is necessary to stop the shaft in the required position, but the accuracy doesn't have to be great. Then the actuator similar to accumulator screwdriver can come out and turn the screw on which the eccentric is mounted on.

This solution seems to be quite inexpensive, simple and acceptable even for larger devices then the calculations are done for. For example, for a common screw M8 when loaded with 1 kN the pressure on the screw is 28,8 MPa and the pressure in the thread is 13,3 MPa which is acceptable and relatively safe.

### **6.3 Drive**

With the drive the greatest problem is the instability in angular velocity. Although on the model this problem wasn't that much seen at the experiment it was. Here are the possible solutions.

1)

First and the simplest solution is strongly over sizing the drive. The drive will then have significantly larger torque than is the maximal load moment. That will make the effects of unstable rotation insignificant and instability will be smaller.

But such solution is not economical and is highly impractical. The only benefit of this solution is its simplicity. For illustration in picture 609 is an example of big DC motor with 22 kW power. Its length is almost 1 meter and weight over 160 kilograms.

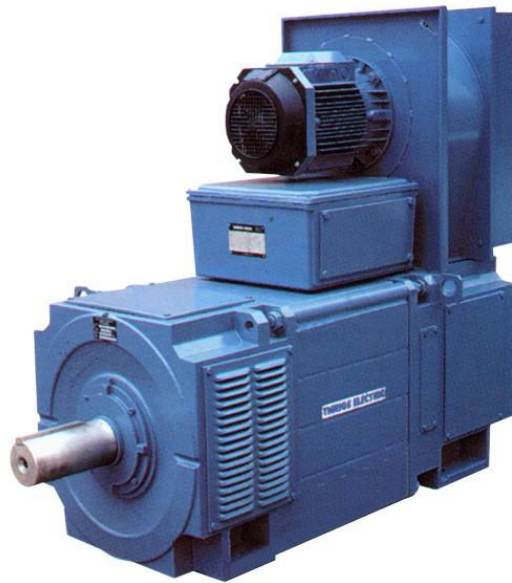


**Fig. 609 – Big DC motor [18]**

2)

Another possible solution is adding a flywheel. The size of flywheel is determined based on instability of operation. Given that for each frequency the instability would be quite different than also the flywheel would have to be significantly oversized.

The benefit of this solution is that it is inexpensive and simple. However, the downside is going to be the time of reaching required rotations which increases with the size of the flywheel.

3)

The best solution would be using adequate control. Predictive regulator would probably be the best. From the mathematical model of the drive can be calculated needed action interference. If we set the model so that the angular velocity is constant, required changes in voltage for keeping it so can be calculated and this will serve as a signal for input. Other unmodeled disturbances can be solved with a feedback.

The drive itself can be described with these equations:

$$\frac{di}{dt} = \frac{1}{L}(U + Ri + k_m \omega) \quad (6.1)$$

$$J \frac{d\omega}{dt} = k_m i - M_L \quad (6.2)$$

Where U is voltage on the armature, R is the resistivity of the armature and L is inductance of the armature,  $k_m$  is constant of motor, J is rotational inertial mass and  $M_L$  is all loads on motor. This load can be calculated from the mechanical part of the system.

When we add to the equations the requirement on constant angular velocity, then the left side of equation 6.2 will become zero and the term for current can be expressed from the equation. When we substitute for the current and its derivation in the equation 6.1 we will get relation for calculating the current increase for keeping the angular velocity constant:

$$U = R \frac{M_L}{k_m} + \frac{L}{k_m} \frac{dM_L}{dt} - k_m \omega \quad (6.3)$$

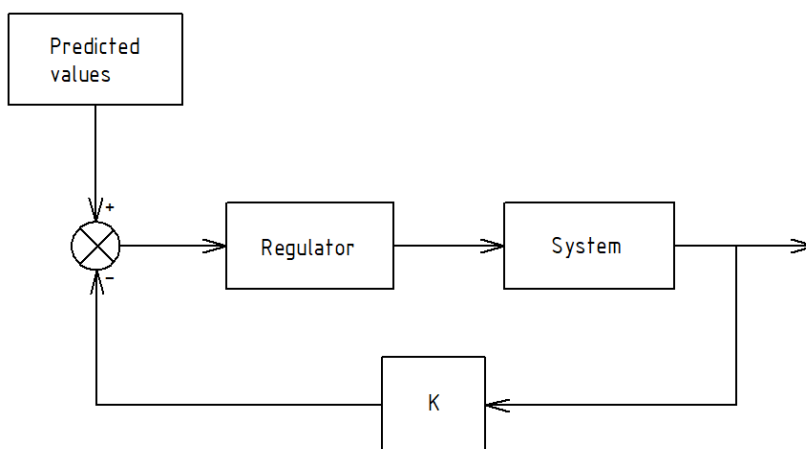


Fig. 610 – Illustrative diagram of system build with control

As a regulator with a feedback could be used LQR regulator. However, we would mustn't forget to linearize the setting with each change.

Sampling frequency in the whole system is also important. Generally, there are no fixed rules of what the sampling frequency should be when it comes to control. The minimum is given by the sampling theorem and also the stability conditions of discrete system. But this do not have to ensure satisfactory quality of regulation. In the literature can be found recommended values. For precise measurement these values are 500 $\mu$ s and less. Given that the system should operate on frequency up to 50 Hz the sampling period could be higher. If we take for example twenty times the maximal frequency, which is usually enough, the sampling period could be 1 ms. But it is always better to check the sampling frequency with simulation.

This solution is very elegant because it can be implemented into the control system of the shaker and doing so will speed up the whole process of measurements. Nonetheless setting this solution is much more arduous then the previous options.

## **6.4 Design summary**

Before deciding on the final design, it is always necessary to consider how the device is going to be used. For the parameters assumed in this thesis we chose combinations of the previously described options:

For the eccentric the solution is going to be bearing with a housing which is the most effective. The shaft of the drive would be connected to the exciter via belt transmission. Given the small eccentricities the solution "eccentric in eccentric" seems as the best alternative even for its complexity. If there was the problem with instability in angular velocity we would choose the predictive control.

## 7. Conclusion

In the research part of the diploma were presented facts about modal analysis. Important were namely information about requirements on excitation for modal analysis. Next were introduced different kinds of exciters and their properties and physical principles.

In the following practical and experimental part was designed small exciter on mechanical principle. From the experiments it became clear the concept itself is possible, but it has its shortcomings. But that was expected. A certain construction changes had to be made and better model of the system had to be implemented.

Then the findings from experiments were used for the optimization. During this optimization was used more complex model of the whole system which was the first step. In the first stage of the optimization was described a method for determining the initial and boundary parameters and also was described the objective function. From this came the discovery that using subresonance solutions is not ideal for larger masses as it generates too big loads on the system. Nonetheless for our experimental exciter this solution seemed to work because the masses were small. For the optimization was used suprapresonance solution with very small main stiffness's.

In the following stage were done two optimizations. First to optimize five parameters in the given frequency range and based on that was determined the main stiffness  $k$  for mounting of the table and ideal mass of the table  $m_0$ . These two parameters were then used in the second optimization as constants. In the second optimization were then optimized parameters for eccentricity  $e$ , predeformation of the spring  $r_0$  and stiffness of spring  $k_b$ . The resulting values were then used for setting the exciter for the test. Exactly this setting is important for fulfilling the main requirement – ensuring the constant acceleration on mass  $M$  and therefore constant excitation force for all needed frequencies. The device must be able to change its parameters for each tested frequency.

In the last part of the optimization were then the outputs tested on a complex model of the exciter where the drive was included. Control was not part of the drive but for

confirming the values the model was satisfactory. The testing showed that the system as a whole operates as it was expected.

In the final part of this thesis were presented concepts of possible designs and solutions to some construction problems and also to setting the parameters of the shaker.

Proposed methods allow us to determine optimal values for exciter in required frequency range, accelerations/exciting forces and sizes of the tested objects. In similar way are proposed some possible designs of the whole shaker.

# Reference

- [1] *ModalAnalysis* [online]. Siemens PLM Software. Germany: Siemens, 2016 [vid. 2016-05-04]. Availablefrom:  
[https://www.plm.automation.siemens.com/en\\_us/plm/modal-analysis.shtml](https://www.plm.automation.siemens.com/en_us/plm/modal-analysis.shtml)
  
- [2] *ModalTesting* [online]Wikipedia. [vid.4-5-2016]. Availablefrom:  
[https://en.wikipedia.org/wiki/Modal\\_testing](https://en.wikipedia.org/wiki/Modal_testing)
  
- [3] MCCONNELL, Kenneth G. a Paulo Sérgio. VAROTO. *Vibrationtesting: theory and practice*. 2nd ed. Hoboken, N.J.: John Wiley, c2008. ISBN 04-716-6651-3.
  
- [4] PAZDERA, Pavel. *Mechanical exciter for modal analysis*. BRNO, 2007. DIPLOMA THESIS. BRNO UNIVERSITY OF TECHNOLOGY. Supervisor: Doc. Ing. IVAN MAZUREK, CSc.
  
- [5] *Opis* [online].OPIS [cit. 4-5-2016]. Availablefrom:  
<http://www.opis.cz/visam/obr/spc.jpg>
  
- [6] *Aliasing*[online].NATIONAL INSTRUMENTS. [vid. 05-16-2016].  
Availablefrom: <http://zone.ni.com/reference/en-XX/help/370051M-01/cvi/libref/analysisconcepts/aliasing/>
  
- [7] STRUM, Robert D. and KIRKDonald E. *Contemporarylinearsystemsusing MATLAB*. PacificGrove, Calif.:Brooks/Cole, c2000. Book Ware companion series (PacificGrove, Calif.). ISBN 05-343-7172-8.
  
- [8] *Fast Fourier transform* [online].Wikipedia. [vid. 2016-05-17]. Availablefrom:  
[https://en.wikipedia.org/wiki/Fast\\_Fourier\\_transform](https://en.wikipedia.org/wiki/Fast_Fourier_transform)
  
- [9] BRANDT, Anders. *Noise and vibrationanalysis: signalanalysis and experimentalprocedures*. Chichester: Wiley, 2011. ISBN 978-0-470-74644-8.
  
- [10] STEINBAUER, Pavel. *Základyinženýrskéhoexperimentu 3* [Lecture]. PRAGUE: CTU in Prague, academic year 2017/2018



- [11] BILOŠOVÁ, Alena. *Aplikovaný mechanik jakosoučást týmu konstruktérů a vývojářů: část modální zkoušky*. Vysoká škola Báňská–Technická univerzita Ostrava.[Online] [vid. 5-8-2018.]. Aviable from:  
<http://projekty.fs.vsb.cz/147/ucebniopory/978-80-248-2758-2.pdf>
- [12] MILÁČEK, Stanislav. *Modální analýza mechanických kmitů*. Praha: ČVUT, 1992. ISBN 80-01-00872-X.
- [13] ČIPERA, Stanislav. *Řešené příklady z matematiky 3.Vyd. 2., přeprac.* Praha: České vysoké učení technické v Praze, 2008. ISBN 978-80-01-04029-4.
- [14] WALTER, Vincent. *Experimental Modal Analysis practically speaking* [Lecture], PRAGUE: CTU in Prague, 19.4. 2018
- [15] *Fmincon*[online]. The MathWorks . United States, c1994-2018 [vid. 08-06-2018]. Aviable from: <https://www.mathworks.com/help/optim/ug/fmincon.html>
- [16] SOBOTKA, Petr. *The implementation of algorithms for experimental modal analysis*. Prague, 2012. Bachelor Thesis. Czech Technical University in Prague. Supervisor STEINBAUER Pavel.
- [17] *Vzduchová pružina SOR zadní náprava*. [online]. AIR SPRINGS – CZ s.r.o.: Váš specialista na vzduchové pérování. Czech republic: Kodak jaboube.cz, 2018 [vid. 09-08-2018]. Aviable from:  
<http://vzduchovepruziny.cz/produkt/vzduchova-pruzina-sor-zadni-naprava/>
- [18] DC Motors. INVERTER DRIVE [online]. Gloucestershire: Inverter Drive Supermarket, 2018 [vid. 10-08-2018]. Aviable from:  
<https://inverterdrive.com/group/Motors-DC/22kW-DC-Motor-TT-Electric-1800RPM-30HP-shunt/>

# List of figures

Fig. 201 - Visualisation of modal decomposition	11
Fig 202 - SDOF Model	13
Fig. 203 - MDOF system	14
Fig. 204 –Simple exhibition of structure of experimental set up for EMA	16
Fig 301 - Impact hammer	19
Fig. 302 - Experimental equipment of company Robert Bosch GmbH	20
Fig. 303 -Vibrational motor with open chamber for unbalance mass	21
Fig. 304 - Direct-drive shaker a) crank b) eccentric	22
Fig. 305 - Piezo actuator for modal excitation with connection element	23
Fig. 306 - Principle diagram of electrodynamic exciter	24
Fig. 307 –Showcase of electrodynamic exciters	24
Fig. 401- Global view on 3D model of shaker	28
Fig. 402 - Inside view of 3D model with description point	29
Fig. 403 - Sketch of physical model of shaker	30
Fig. 404 - Photos of the real model	31
Fig. 405 - Free-body diagram	32
Fig. 406 - Measurement arrangement - a) block schema b) real situation	34
Fig. 407 - DFT of acceleration (left) and audio (right)	36
Fig. 408 - DFT of not absolutely clear signal	37
Fig. 409 Table of slope of increasing power from every frequency and single mass .....	37
Fig. 410 - Spectrum with filters	38
Fig. 411- Approximation of data from accelerometer in CF tool	39
Fig. 412 - Approximation of filtered signal of acceleration and model of acceleration .....	40
Fig. 501 –Sketch of full model	42
Fig. 502 – Free-body of the modified system	43
Fig. 503 - Equilibrium point and its Free-body	45

Fig. 504 - Graphs of acceleration and displacement	54
Fig. 505 – Graphs of minimal and maximal normal force	55
Fig. 506 – Graphs of eccentricity and predeformation	55
Fig. 507 – Graphs of stiffness $k$ and $k_b$	56
Fig. 508 – Graph of weight of table	56
Fig. 509 – Graphs of acceleration and displacement	57
Fig. 510 – Graphs of minimal and maximal normal force	58
Fig. 511 - Graphs of eccentricity and predeformation	58
Fig. 512 – Graph of stiffness $k_b$	59
Fig. 513 – Sketch of model and its free-body	60
Fig. 514 - Graph of motor state variables	63
Fig. 513 – Graphs of acceleration and normal force 50 Hz	64
Fig. 514 – Graphs of acceleration and normal force 10 Hz	65
Fig. 601 – Eccentric cam	67
Fig. 602 – Eccentric with bearing housing	68
Fig. 603 – Air spring	69
Fig. 604 – Illustration of concept with angular transmission	70
Fig. 605 – Illustration of concept with belt transmission	71
Fig. 606 – Illustration of concept with linear drive	72
Fig. 607 – Illustration of concept Eccentric in eccentric	73
Fig. 608 – Illustration of concept with setting screw	74
Fig. 609 – Big DC motor	75
Fig. 610 – Illustrative diagram of system build with drive	76

# Appendix A

## Aliasing

Every signal which is recorded is sampled with some sampling frequency  $f_s$ . If  $f_s$  isn't suitable (large enough), then signal is aliased, and result is poor information. In picture 1 is shown adequately sampled signal (1a) and aliased signal (1b).

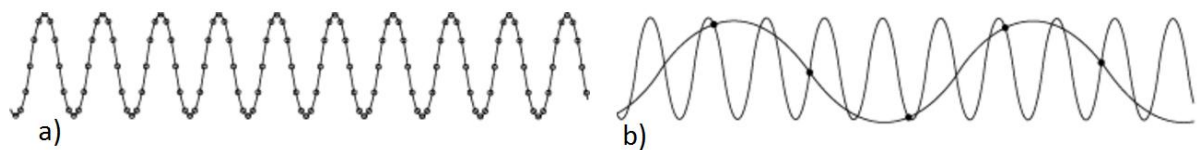


Fig. 1 - Sampled signal - a) Adequately sampled signal b) Aliased signal due to undersampling [6]

If an analog signal has maximal frequency  $f_{\max}$ , the signal can be uniquely represented by equally spaced samples if the sampling frequency  $f_s$  is greater than  $2f_{\max}$ .

The minimum acceptable sampling frequency,  $2f_{\max}$  is known as the Nyquist frequency.[7]

For practical use it is typical to use  $f_s$  which is between  $5f_{\max}$  and  $10f_{\max}$ .

## Anti-aliasing filter

Very easy way how to protect measurement from aliasing is using anti-aliasing filter. It is lowpass filter with maximal pass frequency which satisfy to Nyquist frequency.

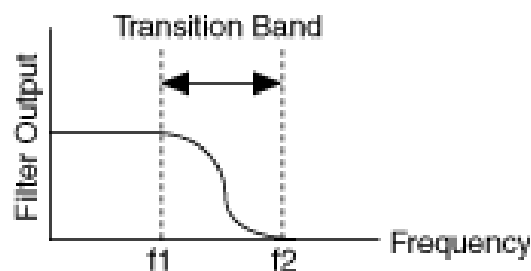


Fig. 2 Antialiasing (lowpass) filter [6]

In picture 2 is frequency response of anti-aliasing filter. This picture illustrates actual anti-alias filter behavior. Practical anti-alias filters pass all frequencies less than  $f_1$  and cut off all frequencies greater than  $f_2$ . The region between  $f_1$  and  $f_2$  is the transition band, which contains a gradual attenuation of the input frequencies. [6]

## Increasing Sampling Frequency to Avoid Aliasing

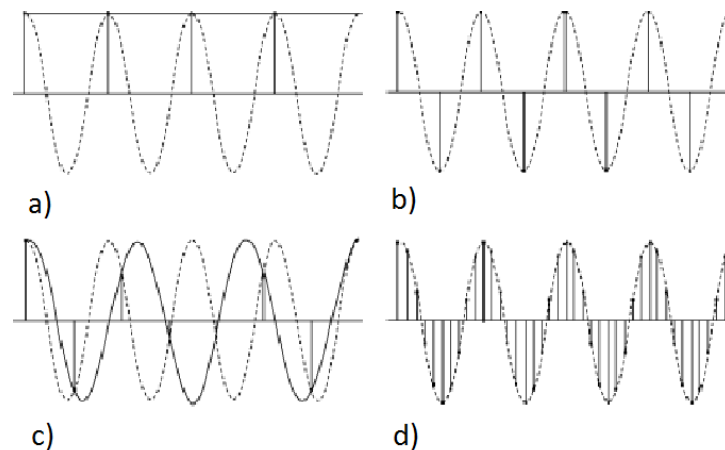


Fig. 3 - Sampled signal with different sampling frequency [6]

In picture 3 is demonstrated the effect of different sampling frequency very well. In part a) is  $f_s=f_{\max}$  and the result is absolutely changed signal - only line.

In part c) is  $f_s=7/4f_{\max}$ . The signal is shifted. If we will follow only discrete points on the wave, the spacing between them and if we approximate the wave using only straight lines (not shown in the picture) we can clearly see that the amplitude of the signal has also changed.

In part b) is  $f_s=2f_{\max}$ . It is possible to see, signal have right amplitude, but it is not represented very well. The result is right frequency and amplitude.

In part d) is  $f_s=10f_{\max}$ . Signal is represented very well, with right frequency, amplitude and very nice curve.

## Digital Fourier transform (DFT/DTFT)

This is a discrete transform which deals with finite sequence of discrete time signal and is very similar to (or it is equivalent of) continuous Fourier transform. Also, it is possible to say it is one of the primary tools of signal processing and study and it enables to find frequency spectrum of a signal (to do spectral analysis).

### DFT

If we have a sequence  $x(n)$  that is nonzero only for finite number of samples in an interval  $0 \leq n \leq N-1$  and we choose to represent the sequence only over this interval, then, the analysis relationship is given by:

$$X(k) = \sum_{n=0}^{N-1} x(n)e^{-j\frac{2\pi}{N}nk}; k = 0,1,2, \dots, N - 1 \quad (7)$$

where  $X(k)$  is referred to as the Discrete Fourier Transform of  $x(n)$ .

## IDFT

The inverse Discrete Fourier Transform (IDFT), or synthesis relationship is given by:

$$x(n) = \frac{1}{N} \sum_{k=0}^{N-1} X(k)e^{j\frac{2\pi}{N}nk} \quad n = 0,1,2, \dots, N - 1 \quad (8)$$

The index  $k$  corresponds to the frequency. The associate values of  $k$  with analog frequency will be described later.

Another version of notation used is:

$$X(k) = DFT[x(n)] \text{ and } x(n) = IDFT[X(k)]$$

Or, in familiar pair notation

$$x(n) \Leftrightarrow X(k)$$

Final insights:

- The DFT is generated by a finite sum and consists only of  $N$  frequency values.
- The IDFT is periodic in  $k$  with period equal  $N$ .
- The DFT representation of  $x(n)$  is periodic in  $n$  with a period equal to  $N$ .
- The DFT values, the  $X(k)$ 's, for a finite-duration sequence are the values that would be obtained by sampling the DTFT  $X(e^{j\theta})$  of the sequence with values of  $\theta$  equal to  $2\pi k/N$ . [7]

The digital frequency  $\theta$  is also used for transforming the continuous time function to sequence:

$$\theta = 2\pi \frac{f}{f_s} \quad (9)$$

Where:  $f$  is frequency of continuous signal and  $f_s$  is sampling frequency. Validity of this relation will be shown later.

## **Cooley–Tukey algorithm**

By far the most commonly used FFT is the Cooley–Tukey algorithm. This is a divide and conquer algorithm that recursively breaks down a DFT of any composite size  $N = N_1N_2$  into many smaller DFTs of sizes  $N_1$  and  $N_2$ , along with  $O(N)$  multiplications by complex roots of unity traditionally called twiddle factors (after Gentleman and Sande, 1966).

This method (and the general idea of an FFT) was popularized by a publication of J. W. Cooley and J. W. Tukey in 1965, but it was later discovered that those two authors had independently re-invented an algorithm known to Carl Friedrich Gauss around 1805 (and subsequently rediscovered several times in limited forms).

The best-known use of the Cooley–Tukey algorithm is to divide the transform into two pieces of size  $N/2$  at each step and is therefore limited to power-of-two sizes, but any factorization can be used in general (as was known to both Gauss and Cooley/Tukey). These are called the radix-2 and mixed-radix cases, respectively (and other variants such as the split-radix FFT have their own names as well). Although the basic idea is recursive, most traditional implementations rearrange the algorithm to avoid explicit recursion. Also, because the Cooley–Tukey algorithm breaks the DFT into smaller DFTs, it can be combined arbitrarily with any other algorithm for the DFT, such as those described below. [8]

### ***Sampling period***

This period must satisfy to sampling frequency  $T=1/f_s$ . Samplings frequency must satisfy to frequency of recorded signal. This problem is discussed in part about aliasing.

### ***Frequency resolution $\Delta f$ and record length $T_0$***

Frequency resolution satisfies to analog frequency of signal and  $k$  in DFT. The relation between these two parameters is  $\Delta f = 1/T_0$ .

Rationally  $\Delta f$  must satisfy to  $f$  or necessary accuracy required.

### ***Number of samples***

Number of samples N is giving length vector of sampled signal:

$$N = T_0 f_s = \frac{T_0}{T} \quad (10)$$

Summarization of equations:

$$T_0 = NT = \frac{N}{f_s} \quad (11)$$

$$\Delta f = \frac{1}{T_0} = \frac{f_s}{N} \quad (12)$$

$$k = \frac{f}{\Delta f} \quad (13)$$

Displaying equations of digital frequency:

$$\theta = \frac{2\pi k}{N} \text{ substitute } k \text{ from equation (13)}$$

$$\theta = \frac{2\pi f}{N \Delta f} \text{ substitute } N \text{ from equation (11)}$$

$$\theta = \frac{2\pi f}{T_0 f_s \Delta f} \text{ substitute } T_0 \text{ from equation (12)}$$

$$\theta = \frac{2\pi}{\Delta f f_s} \frac{f}{\Delta f} = 2\pi \frac{f}{f_s}; \text{ this satisfies the equation (9).}$$

In computersoftware (Matlab, Mathcad, Octave, ...) it is possible to calculate DFT. For calculations is typically used some fast Fourier transformation (FFT) algorithm.



There are many types of FFT algorithm e.g. Rader's algorithm, Prime-factor FFT algorithm, Bluestein's FFT algorithm but the most common is Cooley–Tukey algorithm.

## Spectral leakage

Leakage is a phenomenon when the energy at the single frequency in the sequence spills over, or leaks, into the other frequencies. Typically, this is consequence of the fact that the numbers of points in the DFTs are not integer multiples of the period of the signal. It is also commonly caused by sudden discontinuous changes in the signal.

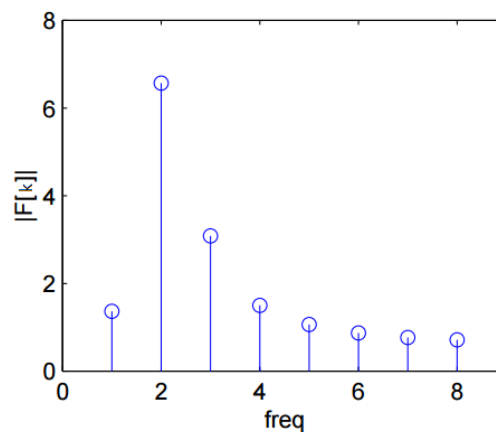


Fig. 4 - Frequency spectrum with leakage

In picture 4 is possible to see non-zero components around the maximal peak (point 2). This is typical example of how of leakage.

To suppress this phenomenon, it is possible to use Hamming or Hanning window function. In picture 5 is frequency spectrum of the same signal as in picture 4 but with using Hanning window.

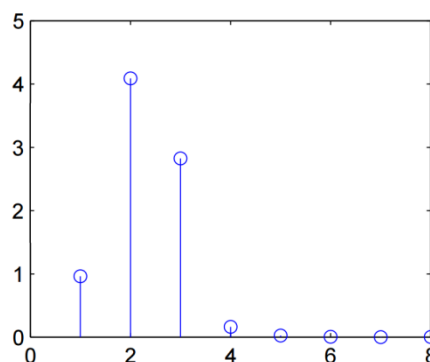


Fig. 5 - Frequency spectrum with leakage after using Hanning window

Thanks to using window function the leakage was suppressed, and peaks are only very close to the correct location of frequency of the signal.

In picture 4 and 5 the leakage is relatively small but in real noise signal it can be much more serious, and information derived from the spectrum are not clear.

It is necessary to point out, that there are many window functions which can be used for suppression of these problems or mistakes in signal e.g. in audio recording/processing.